UCRL-83438
PREPRINT

STATISTICAL ANALYSIS OF GOLD BRIDGEWIRE DISSOLUTION IN DETONATORS AT STORAGE TEMPERATURE

W. J. Siekhaus

This paper was prepared for submittal to the proceedings of the 7th DOE Compatibility Meeting, Savannah River Laboratory, Aiken, SC., October 16-18, 1979.

December 6, 1979

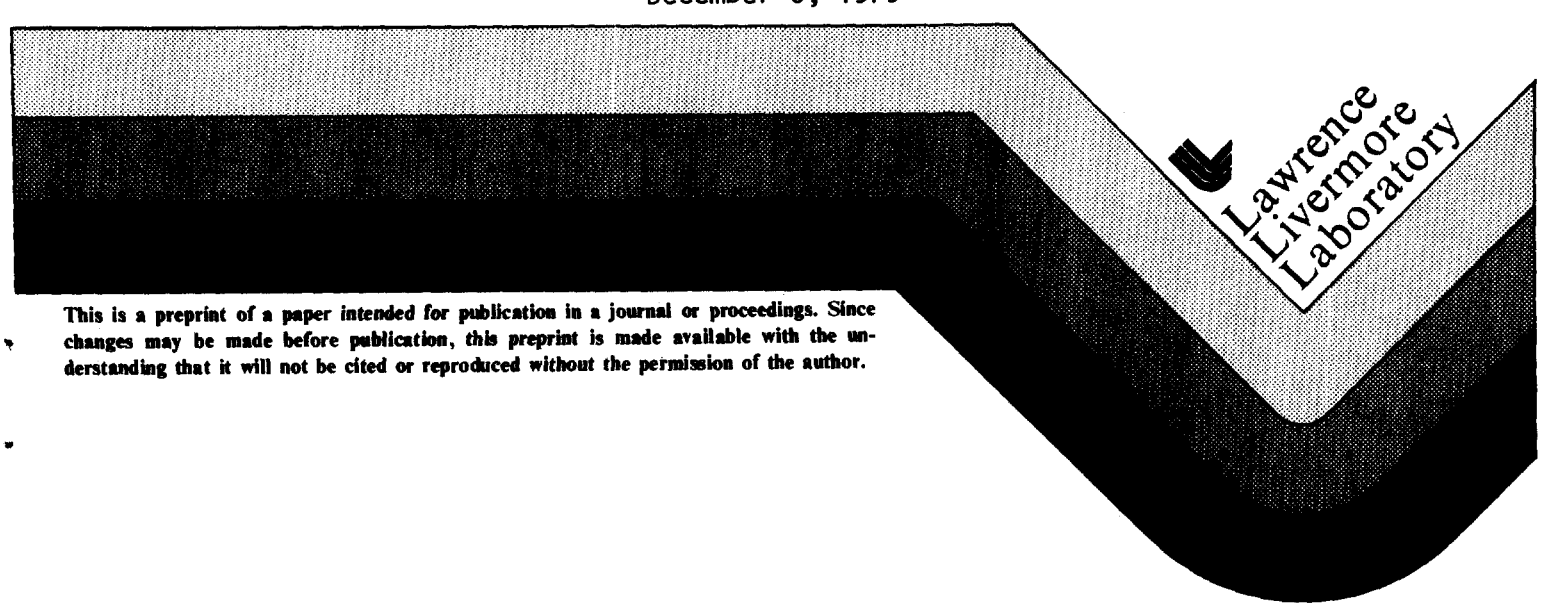

STATISTICAL ANALYSIS OF GOLD BRIDGEWIRE DISSOLUTION IN DETONATORS AT STORAGE TEMPERATURE*

W. J. Siekhaus

December 6, 1979

Abstract

The dissolution data of gold bridgewires held at ambient stockpile storage temperature for up to twenty years are analyzed. The objective is to determine the time dependence of the dissolution at storage temperature. It is shown that these data do not allow us to distinguish with reasonable certainty between different possible time dependencies ($t^{\frac{1}{2}}$ or t). A comparison is then made with dissolution data collected from experiments performed at elevated temperature and the conclusion is made that the dissolution process is proportional to time at room temperature. This mechanism leads to conservative lifetime predictions.

Presented at the 7th DOE Compatibility Meeting, Savannah River Laboratory, Aiken, SC, Oct. 16-18, 1979

*Work performed under the auspices of the U.S. Department of Energy at Lawrence Livermore Laboratory under contract W-7405-Eng-48.

INTRODUCTION

Lifetime predictions for weapon systems using gold bridgewire detonators may depend on reliable estimates of the rate of gold bridgewire dissolution. This gold dissolution is due to the formation of In_2Au in the solder mounds of detonators. A good estimate can be made if the dissolution rate can be described in analytical form. This functional form may be derived from experimental data at several elevated temperatures, with the assumption that extrapolation to storage temperature is possible; alternately, one may deduce a dissolution law from measurements performed on detonators after disassembly of weapons held at storage temperature for long times.

W. D. Harwood[1] used a limited amount of data vailable to him (9 data points) and concluded that the observed reduction in wire diameter in solder mounds at room temperature was consistent with a $t^{\frac{1}{2}}$ law, characteristic of boundary movement between two phases (Au and In_2Au) when the phase growth is diffusion controlled.[2] Siekhaus, et al.,[3] on the other hand, have reported that all known high temperature (>50C) data on In_2Au formation in the thickness range of 0-20 micron can be fitted very well to a rate law proportional to time, typical for interface controlled reactions. This applies equally well to cylindrical and to planar geometry. They also note, however, that at 140C the rate of growth of In_2Au above 70 micron thickness is diffusion controlled. These observations lead to the speculation that the same process which leads to diffusion control in thick layers at high temperature induces diffusion control at low temperature in thin In_2Au layers. If this were so, then the extrapolation of high temperature data to storage temperature conditions would result in misleading lifetime predictions. To resolve this question, we want to look very carefully at all available weapons disassembly data which report In_2Au growth after a known time at storage conditions. R. Yactor of LASL has provided the author with a large body of gold wire dissolution data accumulated from weapon disassembly information over many years and covering many weapon systems.

This report will use this information and try to deduce from it whether gold dissolution is diffusion controlled (i.e., proportional to $t^{\frac{1}{2}}$) or interface controlled ($\approx t$) at weapon storage temperature.

DESCRIPTION OF DATA

Almost all data used in this report were provided by R. Yactor of LASL. Some results came from Janco and Braun[4] and J. D. Braun and T. B. Rhinehammer.[5] The data are presented in this report in two forms. Tables IA to VA give a list of the amount of gold wire dissolution at weapon disassembly time, each table covering one weapon system. Figure 1A shows a graph of all room temperature data; the individual weapon system is identified by a particular symbol. In Figure 1A the decrease in gold bridgewire radius is plotted as a function of age. This decrease is calculated from the value of remaining gold wire area listed in the tables. Figure 1A-a presents the same data on double logarithmic paper and a lower and upper bound to the data is sketched in. The data cover a time span from 25 to 240 months and a gold wire radius reduction due to dissolution from 0.4 to 9 microns. The initial radius of the gold wire is 19.05 microns. These data represent many different weapons (W25, W31, W53, B28, B61) and production times from 1957 (W25) to 1970 (B61). It is apparent that all data points for times less than 140 months are from the B61; W53 data lie almost exclusively (exception: two data at 224, two data at 232 months) between 140 and 180 months; all W31 together with most of the W25 and B28 data fall between 185 and 225 months.

Despite the large total number of points (246) there is not a single weapon system that has data from age zero to age 240 months. In order to arrive at representative long-term behavior, one must treat all data as if they belonged to the same class even though there are probably storage temperature differences between the different weapon systems. Nevertheless, we will look first at some systems individually in order to detect pecularities or inconsistencies.

INDIVIDUAL WEAPONS

1) B61

In Figure 2A, all B61 data are plotted on normal probability paper. Reduction in radius (ΔR) is plotted against cumulative frequency in each age group. As Figure 1A shows, all data corresponding to ages below 130 months come from B61. These, then, define the initial conditions. At an age of 25 months there is very little scatter in gold dissolution thickness, the slope of a line through the data would be almost 90^{0}. At 72 months and at 81 months of age, there is a pronounced break in the distribution. The discontinuity in ΔR between the upper and the lower cluster of data is approximately 0.6 micron. This means that two different populations are being plotted. It is tempting to correlate this difference with the soldering technique used: the gold wire is first provisionally soldered to post one and then carefully aligned with and soldered to post two; thereafter, post one is unsoldered and the wire aligned while the solder is held liquid. Post one is, therefore, subject to much longer heat exposure. The data points are indeed structured so that one low and one high data point always occurs on the same detonator (see B61 table). This conclusion is only very tentative: two age groups with a total of 12 data points do not clearly show it and two age groups with a total of 20 data points do show it. If such an initial differentiation between solder mounds indeed exists, it would become less apparent at later ages because of the natural statistical spread of data with age. One can, therefore, not expect confirmation of the speculation from data of older detonators.

2) W53

The W53 data for ages of 143 and 180 months are plotted on normal probability paper in Figure 3A. The corresponding age is listed in months at the side of the data points. Four data points widely separated in age from this group are not plotted (age greater then 220 months). These data do not seem to fall into two different

groups, as was suspected for the B61. Only in one single detonator (Lot 5718, see Table IIIA) are the dissolution values for the two mounds separated by more than 0.5 micron. One can now ask about the quality of the data: Is the observed spread in dissolution values due to the spread in age (143 to 180 months) or is it due to random measuring error in the determination of the dissolution? If random measuring error determines the spread, then detonator age should not determine whether a point lies in the upper or lower dissolution range, i.e., the detonator age values should be randomly distributed over the dissolution values. Figure 3A shows, however, that the average age of the detonators in the upper dissolution range is about 10 months higher than the average detonator age in the lower dissolution range. Ten months is about one standard deviation of the upper and lower population distribution. One can reach two conclusions from this observation: the accuracy of the measurements is better than two microns (the total spread of this sample) and one should make age groups smaller than a 40-month interval.

3) B28

Two data groups have been chosen: ages 159 to 196 months (Figure 4A) and 209 to 238 months (Figure 5A). The analysis of the age distribution again shows in both cases that the older detonators are found in the upper dissolution range with higher probability. This is very noticeable in the data of Figure 5A, which have only a spread of 30 months. It is less convincing in Figure 4A where the oldest detonator (196 months) provides the third and fourth lowest dissolution value.

4) W31

All W31 data are presented in Figure 6A. They cover a range in age from 185 to 225 months. The data do not fit a single straight line. A good fit can only be achieved with two straight lines, each covering approximately 50% of the data. This implies that detonators in the W31 age in two different environments, probably at two different temperatures. To analyze the data in some more detail, Figures 7A and 8A show smaller age groupings, ages 200 to 210 and 210 to 221

months in Figure 7A, and ages 185 to 200 and 200 to 225 months in Figure 8A. The two groups in Figure 7A are again bimodal. In addition, the average dissolution for the age group 200 to 210 months (3.85 micron) is 1.15 micron larger than the average dissolution for the older detonator group. That is physically unreasonable and is inconsistent with the quality of all other data. Indeed, the average for the age group 185 to 200 months (3.3 micron, Figure 8A) is larger than the average for the age group 210 to 220 months (2.7 micron). The age group 222 to 225 months (Figure 8A) is unimodal, and the average dissolution (4.4 micron) consistent with the reported age. It is not possible to deduce from these data the cause of these anomalies. It is clear, however, that W31 is not "normal" (either as a weapon, or in the reporting technique). An attempt was made to see whether certain serial numbers appear preferentially in the upper half of the bimodal distribution. There is no apparent pattern in the serial numbers, probably because the serial numbers are randomly selected. In Figure 7A the 200 to 210 months age group is also analyzed as a lognormal distribution and the fit to the data is acceptable. This fact does not remove the basic inconsistencies in the data that were pointed out above. Since the W31 provides the majority of the data in the higher age bracket, lognormal averaging allows one to use the data without having to use two modes. One does not have enough data to be able to judge which mode one should use in conjunction with data of other weapons.

5) W25

Figure 9A shows all W25 data. The distribution is unimodal, and an age distribution check shows the expected pattern: older detonators appear preferentially in the upper part of the distribution.

ANALYSIS OF DATA

The evaluation of the data for the individual weapons shows that the data are normally distributed with the exception of W31 and B61. The data are generally of good quality but not enough data are available on

individual systems to follow any weapon through most of its age span to reveal details in the evolution of the bridgewire alloying mechanism. This point is exemplified by the least squares fit of straight lines to the radius decrease versus (1) time (Figure 10A) and (2) versus square-root of time (Figure 11A); the parameters of the fit for each weapon are given in Table I. Table I and Figures 10A and 11A show that over the range where the individual weapons have data point the slopes of the least squares fits differ by about a factor of ten. The quality of fit varies by a factor larger than 300. For a particular weapon a comparison between r^2 and $r^2_{\frac{1}{2}}$ gives no clear indication which model might be a better choice. The largest difference is 5% (B61). In the following discussion all data will, therefore, be pooled to study the dissolution of bridgewires as a single group.

Table I. Least squares fit parameters of radius decrease versus (1) time in month ($\Delta R = a + bt$) or (2) square root of time($\Delta R = a_{\frac{1}{2}} + b_{\frac{1}{2}} t^{\frac{1}{2}}$).

Parameter	Weapon				
	B61	W53	B28	W25	W31
a	-.4983	-1.8998	-6.497	-0.0344	2.57677
b	.03101	.030856	.0589	.0203	.00623629
goodness of fit, r^2	.42837	.69229	.467199	.067249	.0018704
$a_{\frac{1}{2}}$	-1.99113	-7.60201	-17.7705	-4.32	1.21425
$b_{\frac{1}{2}}$	.4395	.84176	1.63376	.59	.18448
goodnes of fit, $r^2_{\frac{1}{2}}$	.40693	.68875	.46141	.073	.001986

ANALYSIS OF THE POOLED DATA FROM ALL WEAPON SYSTEMS

The dissolution data are plotted in age groups of not more than 30 months spread in Figures 12A to 18A. On the same graph, the data are analyzed as either normally (lower scale) or lognormally (upper scale) distributed. The lognormal distribution produces a much better fit for the data above 180 months age, as is shown in Figures 17A and 18A. On both these graphs the large data symbols in the high ΔR region where the two lines intersect refer to the normal distribution. Since the lognormal distribution gives a better fit in the upper age range and is an equally good fit to the lower age range, lognormal averages will be preferred in the following treatment. No particular physical mechanism of aging is implied by this choice between the two distributions.

In Figures 19A and 20A normal and lognormal best-fit straight lines through the data points are shown. The age range corresponding to each curve is also shown, as is the number of data points (circled) associated with each curve. The normal distributions show a significant decrease in slope with age; this is physically reasonable, since the spread in the data points increases with the absolute value of the average. For the same reason the slope in the lognormal distributions stays almost constant. The two curves in Figures 19A and 20A which deviate most from this pattern contain only 10 and 12 data points, respectively.

Table II lists the normal and lognormal gold dissolution averages, and in the last six rows shows the parameters of a least squares straight line fit to them. (The curve drawn in Figure 1A corresponds to a lognormal average fit. The data were averaged over ten-month intervals in Figure 1A.) The lognormal analysis gives slightly lower averages in dissolution thickness but the difference is less than 10% everywhere. The slightly lower averages are to be expected since lognormal averaging places less emphasis on high data points.

The least squares fit parameters in the last six rows are generated by weighting each data point with the appropriate number of data points averaged. The first column in the last six rows contains the parameters

Table II. Average gold dissolution in different age ranges. Both normal and lognormal averages are given. The last six rows give the parameter of linear least squares fits to the data.

Number of data points	Age range (months)	Average age	Square-root of the average age	Normal average of $\Delta R(\mu)$	Lognormal average of ΔR (μ)
12	20-49	34.83	5.90	.845	.816
26	50-79	59.92	7.74	1.00	.915
12	80-89	81.17	9.01	2.10	1.876
10	120-149	132.4	11.51	2.90	2.84
28	150-179	166.07	12.89	3.32	3.16
76	180-209	198.43	14.09	4.05	3.775
28 points		197.93*	14.07	4.08	
48 points		199.17†	14.11	4.03	
64	210-238	218.97	14.80	4.562	4.18
30 points		219.47*	14.81	5.48	
34 points		218.53†	14.78	3.654	

	$\sqrt{t}$		t		$\sqrt{t}$	t
r^2	.989013	* .92	.98771	*.87142	.9834	.98771
slope intercept	.449578	* .50	.02066	*.022	.414	.01899
ΔR = 0, t or $\sqrt{t}$ =	-2.227	*-2.71	-.0088	*-.169	-2.03	.022298
t = 200, ΔR =	4.955	* 5.35	.429	*7.64	4.8979	-1.173647
$\sqrt{t}$ = 15, ΔR =	4.49	* 4.88	4.13	*4.25	4.1855	3.82

* = no W31 data included.
† = W31 data only.

for a fit of normal average of Δr versus square-root of time. The next column, preceded by an *, represents the fit of the normal average of ΔR versus square-root of time, but excluding all W31 data. Column 3 shows the parameters appropriate for a least squares fit of the normal average of ΔR versus time. Column 5 deals with the fit of the lognormal average of ΔR versus square root of time; column 6 gives the fit of the lognormal average of ΔR versus time. For all fits which include the W31 data in the averaging procedure, the coefficient of determination, r^2, is high, $>.98$ and differs between all possible choices only in the third digit; the highest number, .989, appears for the fit of the normal average of ΔR versus square root of time; the lowest value, .983, is for the fit of the lognormal average of ΔR versus square root of time. The coefficient of determination is smaller, $<.92$, if W31 data are totally excluded, (* parameters), and the fit of the normal average of ΔR versus square-root of time is again better, this time substantially, (5%). To remove any concern that the error generated by taking the square-root of the arithmetic average age rather than the arithmetic average of the square-root of age might influence the comparison, a least squares fit of all data versus time and versus square-root of time was done. The parameters are:

Table III

$\Delta R = a + bt$		$\Delta R = a + b\sqrt{t}$
	t	$\sqrt{t}$
r^2	.43074	.42700
slope	.0200141	.43257
intercept	.110494	-2.00059986

The absolute value of r^2 is lower, as expected, in this case. The difference, however, is again approximately 1%. The corresponding straight lines are shown under the label "all" in Figures 10A and 11A.

COMPARISON WITH DISSOLUTION OF ELEVATED TEMPERATURES.

It is apparent that the original question: "Are the data consistent with a linear time law or a square-root of time law?" cannot be resolved by these data. We, therefore, examine them in conjunction with the elevated temperature data of J. D. Braun and T. H. Rhinehammer.[5] For this purpose all data are plotted as a function of time in Figure 21A and as a function of square-root of time in Figure 22A. The LASL data are averaged (geometric mean = lognormal average) over 10-month intervals, the Braun and Rhinehammer data are not corrected for any possible initial reaction due to soldering. Neither in Figure 21A nor in Figure 22A can all the data be fit completely with straight lines. Table IV lists the parameters one obtains from linear least squares fit to the dissolution data, assuming that ΔR is either proportional to t or proportional to $t^{\frac{1}{2}}$, or proportional to $\sqrt{(t = t_0)}$, where t_0 is some incubation time. A choice between the different mechanisms cannot be made on the basis of the goodness of fit to the data. The quantity r^2 differs only slightly between the models. (Since the last model in Table IV fits ΔR^2 versus time, all deviations are magnified and a decrease in r^2 is expected.) There is also no discernable trend in r^2 as a function of temperature. One must therefore look to other parameters in order to differentiate between the two models. The parameter a in the fit $\Delta R = a + bt$ increases monotomically with increasing temperature, from .0223 at 20C to 3.47 at 120C. It is not clear exactly how large the dissolution due to soldering at time zero (namely, a) is, but it is certainly less than 1 micron. Experiments at Livermore have shown that a is close to zero under normal soldering conditions. J. D. Braun has not observed dissolution due to soldering,[8] Harwood[1] shows ΔR to be approximately 1 micron after 6 months storage at room temperature, and for all of the

Table IV. Least square fit parameters to the gold bridgewire dissolution data of Braun and Rhinehammer[5] at elevated temperature and the LASL data; ΔR is in μ, t is in months, T in centigrade.

T	20	50	60	70	80	100	120
				$\Delta R = a + bt$			
a	.0223	-.57	.112	.624	1.356	2.34	3.47
b	.0189	.274	.547	.828	1.158	1.81	2.72
r^2	.9877	.996	.9913	.9816	.9912	.998	.9881
				$\Delta R = a_{\frac{1}{2}} + b_{\frac{1}{2}} t^{\frac{1}{2}}$			
a	-2.03	-3.88	-4.07	-3.22	-3.939	-3.624	-2.22
b	.414	2.05	3.08	3.83	5.261	6.9116	8.12
r^2	.9877	.9598	.993	.995	.9802	.978	.9823
				$\Delta R^2 = c(t - t_o)$			
c	.106	2.48	5.44	9.61	20.07	31.79	55.525
t_o	42.7	6.19	3.4	1.62	1.71	.46	.44
r^2	.96	.922	.958	.977	.966	.988	.9686
No. of points	7	6	9	7	9	7	5

B61 data at 25 months ΔR is below 1 micron. If one takes the "reasonableness" of the parameter a as the criterion one must conclude that the dissolution data are fit well by the linear equation only at low temperatures. The parameter $a_{\frac{1}{2}}$ in the equation $\Delta R = a_{\frac{1}{2}} + b_{\frac{1}{2}} t^{\frac{1}{2}}$ is always negative and almost constant. Such behavior is typical for diffusion controlled phase growth delayed by an "incubation time" with an incubation

process having the same activation energy as the diffusion process. Therefore, one cannot reject the diffusion controlled reaction mechanism on the basis of the "unreasonable" coefficient $a_{\frac{1}{2}}$. However, no incubation time has been seen in the careful experiments performed by Yost, et al.,[8] on planar Au-Pb/In (50/50) solder joints. It is, therefore, unlikely that an incubation process occurs in the Au-Pb/Sn/In (37.5/-37.5/25) solder joints, since the reaction products are the same in both cases. This comparison with dissolution observed at elevated temperatures suggests strongly that the dissolution of gold bridgewires in solder mounds is proportional to time.

LIFETIME PREDICTIONS

In Figure 23A the dissolution ΔR in micron at room temperature is plotted versus time in month on double logarithmic paper. The data points are taken from Table II and represent the lognormal average over the data in the age range indicated. Also plotted are the 95% and 99% cumulative probability points derived from Figure 12A to 18A. The least square fits of the two models are also shown. On the right abscissa the percentage of gold wire volume is shown. Clearly, both models represent the data well over the time range of observation, but the model linear with time predicts faster dissolution with time in the future and should, therefore, be used as the basis for any conservative reliability analysis. The estimated 95% and 99% lines are drawn through the points relying on eye judgement only. To illustrate the use of Figure 23, let us determine the probable degree of dissolution of a group of detonators 300 months old. We draw a vertical dashed line at the abscissa 300 months. The intersection of this line with the solid black line indicates that in 50% of all detonators the gold wire radius wil be decreased by less than 6.4 micron (left ordinate) which is equivalent to a dissolution of less than 55% of the gold wire volume (right ordinate). The remaining 50% of all detonators will have higher dissolution, but as we go up along the vertical dashed line we find that in 95% of all detonators the gold wire

radius will have decreased by less than 10 micron (less than 75% volume dissolution). Going up along the dashed vertical line even further, we see that 99% of all detonators will have their gold wire radius decreased by less than 12 micron, which is equivalent to less than 80% volume dissolution. Of course, 1% of all detonators will have a higher degree of dissolution.

CONCLUSION

From a statistical analysis of the dissolution of gold wires in detonators stored at room temperature and at elevated temperatures one cannot determine whether the dissolution is linear with time or with square-root of time. The time dependence may indeed be more complex because substantial rearrangement of the reaction product must occur because of the cylindrical geometry. However, if we assume the dissolution to be proportional to square-root of time, we are forced to accept that there is an incubation time before the reaction starts, a fact which has not been observed in reaction studies with similar solder. It is, therefore, more reasonable to assume that the gold bridgewire dissolution is proportional to time. This assumption leads also to conservative lifetime predictions.

I would like to stress that this analysis deals only with gold wire dissolution within the solder mound. Gold wire dissolution outside the solder mound occurs and will be analyzed in the future.

Acknowledgement

Without the cooperation of R. Yacktor and T. L. Tucker of LASL this report would not have been possible. J. D. Braun of Mound Laboratory carefully researched her files and answered questions concerning soldering procedures. The members of the Compatibility Group of the General Chemistry Division at Lawrence Livermore Laboratory under Herman Leider, introduced me to this problem, and helped with constructive work and critical words.

FIGURE CAPTIONS

Figure 1A. The dissolution of gold bridgewires at storage temperature, ΔR in μ, versus time in month. LASL and Mound Laboratories data are shown.

Figure 1A-a. The dissolution of gold bridgewires at stockpile storage temperatures, $\log \Delta R$ (μ) versus log (time), (month).

Figure 2A. The distribution of the dissolution of B61 gold bridgewires at age 25, 72, 81, and 124 months plotted on normal probability paper. Abscissa, ΔR, is in microns.

Figure 3A. The distribution of the dissolution of W53 gold bridgewires in the age bracket 143-180 months plotted on normal probability paper. The abscissa is in microns. Storage time is noted at each data point to show that the lower part of the distribution contains mainly younger bridgewires.

Figure 4A. The distribution of the dissolution of B28 bridgewires in the age bracket 154-196 months plotted on normal probability paper. The abscissa is in microns. Individual bridgewire age is shown together with the average age in the lower and upper 50% of the distribution.

Figure 5A. The distribution of the dissolution ΔR in microns of B28 gold bridgewires in the age bracket 209-238 months. Age of each data point is shown together with the average age of the upper and lower 50% of the distribution plot is on normal probability paper.

Figure 6A. The distribution of the dissolution ΔR (microns) of W31 gold bridgewires in the age bracket 185-225 months. The plot is on normal probability paper with the abscissa in microns.

Figure 7A. The distribution of the dissolution ΔR (microns) of W31 gold bridgewires in the age brackets 200-210 and 210-220 months The plot is on normal probability paper with the abscissa in microns.

Figure 8A. The distribution of the dissolution ΔR in microns of W31 gold bridgewires in the age brackets 185-200 and 222-225 months.

Figure 9A. The distribution of the dissolution ΔR in microns, of W25 gold bridgewires in the age bracket 193-227 months.

Figure 10A. Graph of the equations $\Delta R = a + bt$, ΔR in microns. Time, t, is in months for the individual weapon systems. The lines and symbols are drawn only over the range where data exist. The parameters a and b were determined by a linear regression fit to the data.

Figure 11A. Graphs of the equations $\Delta R = a_{\frac{1}{2}} + b_{\frac{1}{2}}$ for the individual weapon systems where ΔR is in microns, t is in months. The lines and symbols are drawn only over the range where data exist. The parameters $a_{\frac{1}{2}}$ and $b_{\frac{1}{2}}$ were determined by linear regression.

Figure 12A to Figure 18A. Distribution of bridgewire dissolution data pooled into different age groups: 20-49 months (Figure 12A), 50-79 months (Figure 13A), 80-89 months (Figure 14A), 120-149 months (Figure 15A), 150-179 months (Figure 16A), 180-209 months (Figure 17A), 210-239 months (Figure 18A). The system to which the data point belongs is identified by a characteristic symbol. The data are plotted twice on normal probability paper, once with respect to the lower abscissa (ΔR in micron), once with respect to the upper abscissa ($\log \Delta R$ in micron). Straight lines fits are drawn through the points.

Figure 19A and Figure 20A. All straight line fits to the distributions in the various age brackets are drawn together for comparison in one graph. Figure 19A shows the normal distributions, Figure 20A, the lognormal distributions. The age bracket belonging to each line is indicated, and the number of points making up the line is circled.

Figure 21A. Graph of ΔR (μ) versus time (months). The data of Rhinehammer and Braun[5] are plotted versus the lower abscissa; the data of LASL, geometrically averaged and plotted in the middle of the 10-month interval over which they occurred, refer to the upper abscissa. The number next to the triangular data points refers to the number of data points averaged.

Figure 22A. Graph of ΔR in microns versus square-root of time (months). See caption to Figure 21A.

Figure 23A. The averaged stockpile temperature dissolution data are shown as a function of age, together with the linear and square-root time fits to them. The 95% and 99% confidence points are derived from Figure 12A to 18A. The abscissa is the logarithm of the age in months, the left ordinate is the logarithm of ΔR in microns; the right ordinate is the fraction of the gold wire volume dissolved in percent The 95% and 99% confidence lines are an eye estimate.

REFERENCES

1. William D. Harwood, Gold-Indium Diffusion in Bridgewires, Sandia Laboratories, Albuquerque, NM. SAND 77-0852 (1977).

2. J. Crank, The Mathematics of Diffusion, (Clarendon Press, Oxford, 1975), p 308.

3. W. Siekhaus, et al.,Minutes of the 18th Meeting JOWOG-12, September 18-21, 1978, Los Alamos Scientific Laboratory, Los Alamos, NM, WX-5-79-77 (1979)

4. B. L. Janco and J. D. Braun, "Investigation of Reaction Rate Between Pure Gold and Pb-Sn-In Solder," Metallographical Review (Inf. Metallography Soc.) 2, 16 (1973); and private communication.

5. J. D. Braun and T. B. Rhinehammer, "An Investigation of the Reaction Between Pure Gold Wire and Lead-Tin-Indium Solder," ASM Transactions Quarterly 56, 870 (1963).

6. M. M. P. Janssen and G. D. Rieck, "Reaction Diffusion and Kirkendall Effect in the Nickel-Aluminum System," Transactions Met. Soc. AIME 239, 1373 (1967).

7. G. W. Powell and J. D. Braun, "Diffusion in the Gold-Indium System," Transaction Met. Soc. AIME 230, 694 (1964).

8. F. G. Yost, F. P. Ganyard, and M. M. Karnowsky, "Layer Growth in Au-Pb/In Solder Joints," Met. Trans 7A, 1141 (1976).

APPENDIX

Data Summary

Table 1A. Gold bridgewire dissolution measured at disassembly.

MARK	CYCLE	OPER	LOT	BUILD DATE	DISA DATE	AGE	% GOLD REMAIN	RADIUS DECREASE ΔR, μ
1E30 B61	7	55A	05 61	9/69	9/75	72	79	2.12
							94	0.58
				9/69	9/75	72	84	1.59
							96	0.38
				9/69	9/75	72	81	1.91
							91	0.78
				9/69	9/75	72	79	2.12
							91	0.88
	7	SLT	02 75	5/65	9/75	124	65	3.69
							70	3.11
				5/65	9/75	124	70	3.11
							70	3.11
				5/65	9/75	124	65	3.69
							74	2.66
			03 A7	12/68	9/75	82	36	7.62
							70	2.01
			03 A9	1/69	9/75	81	71	3.00
							75	2.55
				1/69	9/75	81	68	3.34
							68	3.34
			03 B1	1/69	9/75	81	75	2.55
							88	1.18
			03 B2	1/69	9/75	81	77	2.33
							94	0.58
			05 E2	4/70	9/75	81	80	2.01
							90	0.98
1E30 B61		NMLT				25	93	.68
							93	.68
						25	93	.68
							93	.68
						25	.95	.48
							.92	.78
		SLT				36	.9025	.95
							.9025	.95
						49	.9025	.95
							.9025	.95
						49	.856	1.042
							.9025	.95
						51	.9025	.95
							.9025	.95
						53	.9025	.95
							.9025	.95
						53	.9025	.95
							.9025	.95
						53	.9025	.95
							.951	.47
						53	.9025	.95
							.9025	.95
						53	.951	.47
							.9025	.95
						55	.9025	.95
							.9025	.95
						55	.951	.47
							.9025	.95
						65	.9025	.95

Table IIA. Gold bridgewire dissolution measured at diassembly.

MARK	CYCLE	OPER	LOT	BUILD DATE	DISA DATE	AGE	% GOLD REMAIN	RADIUS DECREASE ΔR, μ
1E26 W25	14	SLT	5037	7/57	4/76	225	63	3.93
							62	4.05
			1026	5/57	4/76	227	63	3.93
							68	3.34
			1233	3/59	4/76	205	59	4.66
							53	5.18
			5152	5/58	4/76	215	59	4.41
							57	4.67
			5052	9/57	4/76	223	52	5.31
							51	5.44
			5247	10/58	4/76	210	53	5.18
							55	4.92
1E26 W25	13	SLT	5679	2/62	5/75	159	83	1.69
							78	2.22
			5109	2/58	3/75	205	69	3.22
							70	3.11
			5109	2/58	3/75	205	68	3.34
							68	3.34
			5326	2/59	5/75	195	46	6.31
							51	5.44
			1222	2/59	5/75	195	66	3.57
							67	3.45
			5344	3/59	6/75	195	73	2.77
							69	3.22
			5271	11/58	5/75	198	51	5.44
							57	4.66
1E26 W25	12	SLT	1202	1/59	5/75	196	64	3.81
							64	3.81
			1244	4/59	5/75	193	69	3.23
							64	3.81
			5065	10/65	5/75	211	79	2.12
							72	2.89
			5144	3/59	5/75	205	64	3.81
							63	3.93
			5345	3/59	5/75	194	42	6.70
							44	6.41

Table IIIA. Gold bridgewire dissolution measured at disassembly.

MARK	CYCLE	OPER	LOT	BUILD DATE	DISA DATE	AGE	% GOLD REMAIN	RADIUS DECREASE ΔR, μ
IE26 W53	11	SLT	5166	5/58	9/77	232	58	4.54
							51	5.44
			5306	1/59	9/77	224	47	5.98
							59	5.05
			5708	9/62	9/77	180	70	3.11
							71	2.99
			5727	4/63	9/77	173	65	3.69
							66	3.57
			5738	7/63	9/77	170	66	3.57
							68	3.34
			5767	2/64	9/77	163	65	3.69
							66	3.57
	10		5710	9/62	8/76	167	78	2.22
							78	2.22
			5725	4/63	8/76	160	70	3.11
							66	3.57
			5741	8/63	8/76	156	73	2.77
							73	2.77
	9		5718	12/62	5/75	149	72	2.88
							81	1.91
			5741	8/63	5/75	141	76	2.42
							76	2.42
			5695	5/62	7/75	156	63	3.92
							67	3.46

Table IVA. Gold dissolution measured at disassembly.

MARK	CYCLE	OPER	LOT	BUILD DATE	DISA DATE	AGE	% GOLD REMAIN	RADIUS DECREASE ΔR, μ
1E26 B28	13	SLT	1328	2/60	8/77	210	43	6.56
							45	6.27
			5471	9/59	8/77	215	43	6.56
							47	5.99
			5621	12/60	8/77	218	48	5.85
							51	5.45
			5636	4/61	8/77	196	77	2.33
							75	2.55
			5723	3/63	8/77	173	59	4.42
							68	3.34
			5723	3/63	8/77	173	52	5.31
							55	4.92
			5774	5/64	8/77	159	70	3.11
							69	3.23
1E26 B28	13	SFT	1337	3/60	8/77	209	56	4.79
							51	5.45
			5064	10/57	8/77	238	34	7.94
							37	7.46
			5723	3/63	8/77	173	84	1.59
							84	1.59
			5749	10/63	8/77	166	59	4.42
							59	4.42
1E26 B28	13	RET	1226	2/59	8/77	222	31	8.44
							38	7.31
			1324	1/60	8/77	211	28	8.97
							28	8.97
			5559	1/60	8/77	211	63	3.93
							66	3.57
			5713	11/62	8/77	177	57	4.17
							65	3.69

Table V,1A. Gold dissolution measured at disassembly.

MARK	CYCLE	OPER	LOT	BUILD DATE	DISA DATE	AGE	% GOLD REMAIN	RADIUS DECREASE ΔR, μ
1E26 W31	13	SLT	1198	12/58	3/76	207	69	3.23
							69	3.23
			5261	11/58	3/76	208	72	2.89
							72	2.89
			5319	2/59	3/76	205	70	3.11
							72	2.89
			5325	2/59	3/76	205	59	4.42
							59	4.42
			5339	3/59	2/76	203	77	2.33
							79	2.12
1E26 W31	13	RET	5357	3/59	2/76	203	29	8.79
							37	7.94
1E26 W31	13	SFT	1250	4/59	2/76	202	44	6.41
							39	7.15
			5238	10/58	2/76	208	57	4.67
							55	4.92
			5412	2/59	2/76	204	70	3.11
							75	2.55
			5450	7/59	2/76	199	72	2.89
							74	2.66
			5557	1/60	2/76	193	65	3.69
							67	3.46
			5592	1/60	3/76	194	69	3.23
							68	3.34

Table V,2A. Gold wire dissolution measured at disassembly.

MARK	CYCLE	OPER	LOT	BUILD DATE	DISA DATE	AGE	% GOLD REMAIN	RADIUS DECREASE ΔR, μ
1E26							44	6.41
W31	12	SLT	1143	7/58	3/75	200	56	4.79
							86	1.38
			5483	10/59	3/75	185	85	1.49
							66	3.57
			5461	8/59	3/75	187	65	3.69
							61	3.46
			5361	3/59	3/75	192	52	5.31
							32	8.27
			1176	10/58	3/75	197	37	8.27
							72	2.89
			5417	6/59	3/75	188	73	2.77
1E26							63	3.93
W31	11		5292	1/59	9/75	200	68	3.46
							56	4.79
			5315	2/59	9/75	199	56	4.79
							69	3.23
			5316	2/59	9/75	199	70	3.11
							54	5.58
			5242	9/58	9/75	203	51	5.45
							76	2.44
			5405	6/59	9/75	195	68	3.34

Table V,3A. Gold wire dissolution measured at disassembly.

MARK	CYCLE	OPER	LOT	BUILD DATE	DISA DATE	AGE	% GOLD REMAIN	RADIUS DECREASE ΔR, μ
1E26 W31	14	SLT	1168	9/58	3/77	222	56	4.79
							55	4.92
			1190	12/58	3/77	219	67	3.46
							66	3.57
			1262	5/59	3/77	214	73	2.77
							76	2.44
			1335	3/60	3/77	204	77	2.33
							81	1.91
			5186	6/58	3/77	225	64	3.81
							61	4.17
			5413	5/59	3/77	214	73	2.77
							76	2.44
			5471	9/59	3/77	210	82	1.80
							82	1.80
1E26 W31	14	RET	1170	9/58	4/77	223	44	6.41
							59	4.42
			1175	10/58	4/77	222	66	3.57
							74	2.66
			5227	9/58	4/77	223	56	4.79
							59	4.42
			5231	9/58	4/77	223	49	5.72
							49	5.72
			5232	9/58	4/77	223	72	2.89
							74	2.66
1E26 W31	14	SFT	1209	1/59	4/77	218	55	4.92
							57	4.67
			1220	2/59	4/77	217	67	3.46
							65	3.69
			5328	2/59	4/77	217	76	2.44
							75	2.55
			5352	3/59	4/77	216	74	2.66
							75	2.55
			5385	4/59	4/77	215	49	5.72
							55	4.92
			5395	5/59	4/77	214	78	2.55
							79	2.12

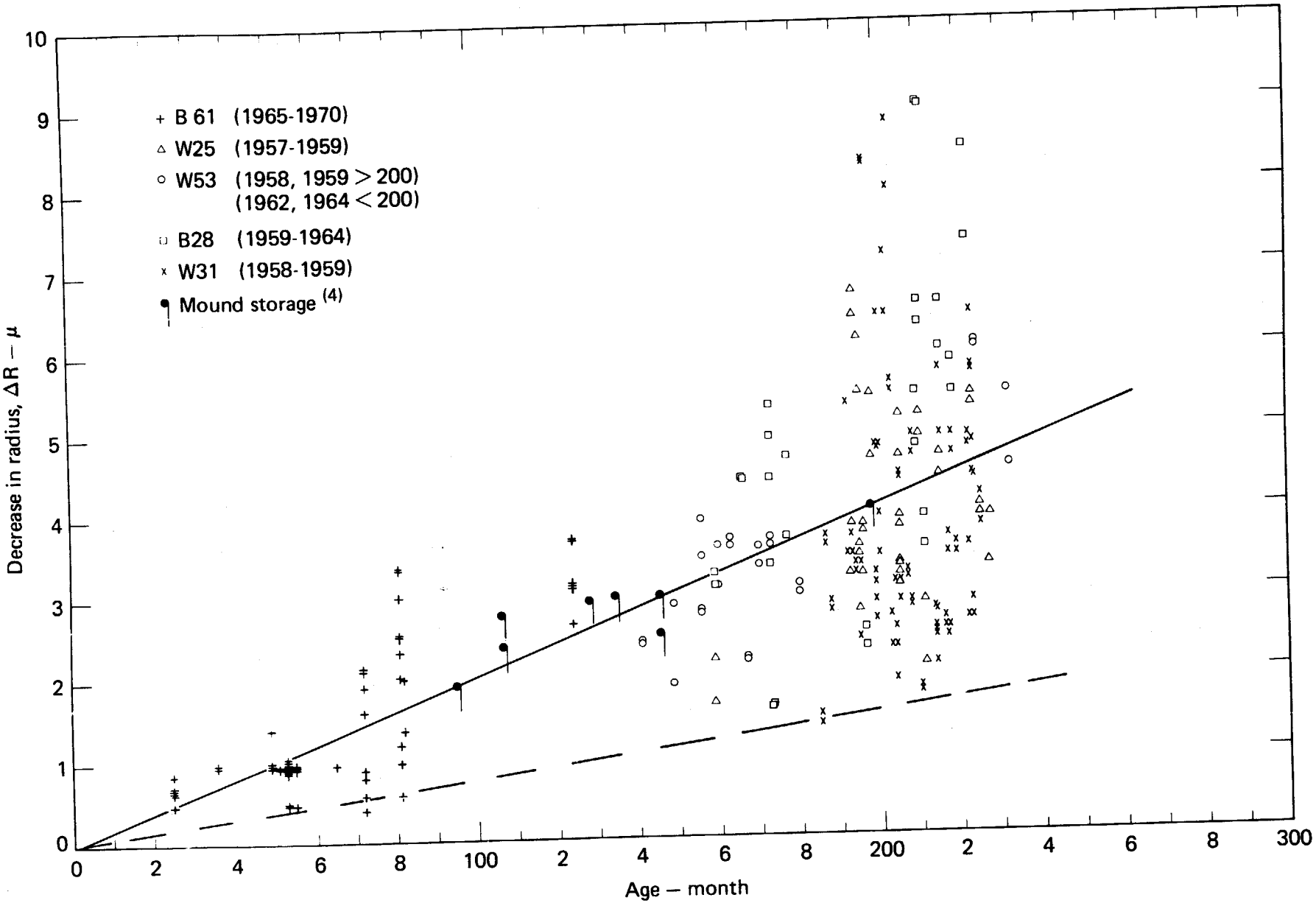
+ B 61 (1965-1970)
△ W25 (1957-1959)
○ W53 (1958, 1959 > 200)
(1962, 1964 < 200)
□ B28 (1959-1964)
x W31 (1958-1959)
Mound storage (4)
Decrease in radius, ΔR – μ
Age – month
0
1
2
3
4
5
6
7
8
9
10
0
2
4
6
8
100
2
4
6
8
200
2
4
6
8
300

FIGURE 1A

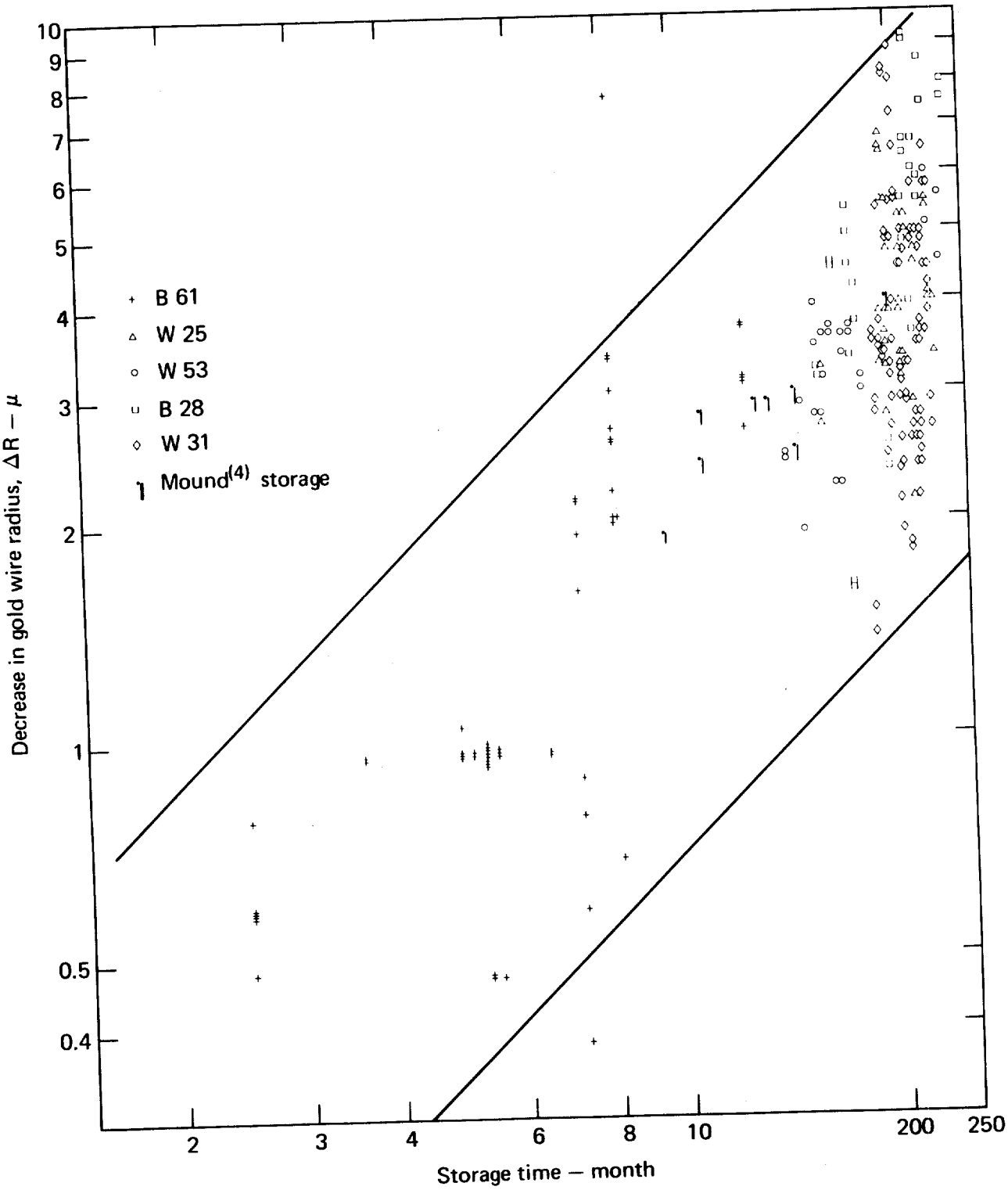
10
9
8
7
6
5
4
3
2
1
0.5
0.4
Decrease in gold wire radius, ΔR — μ
B 61
W 25
W 53
B 28
W 31
Mound(4) storage
2
3
4
6
8
10
200
250
Storage time — month

FIGURE 1A-a

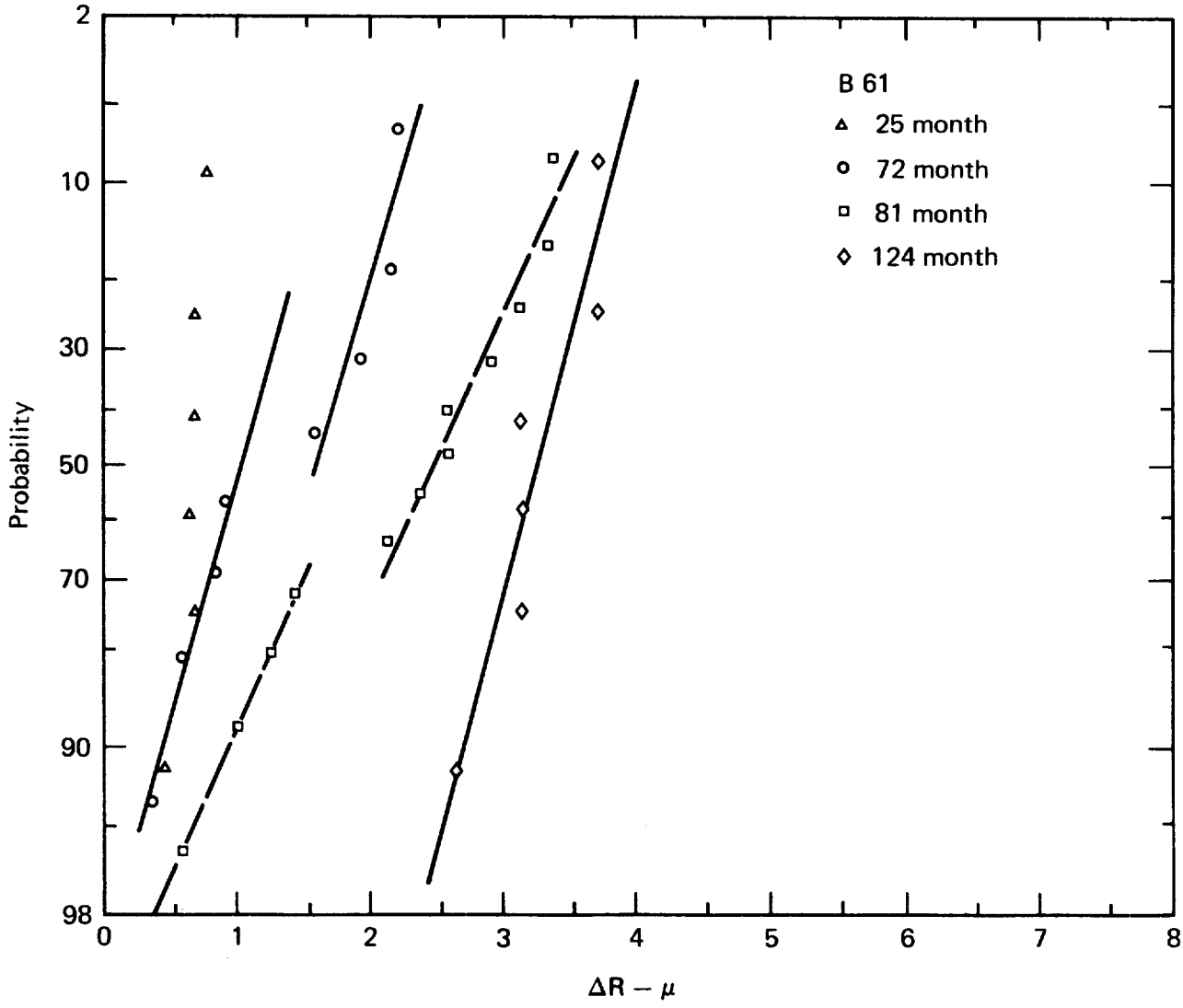
B 61
25 month
72 month
81 month
124 month
Probability
2
10
30
50
70
90
98
0
1
2
3
4
5
6
7
8
ΔR − μ

FIGURE 2A

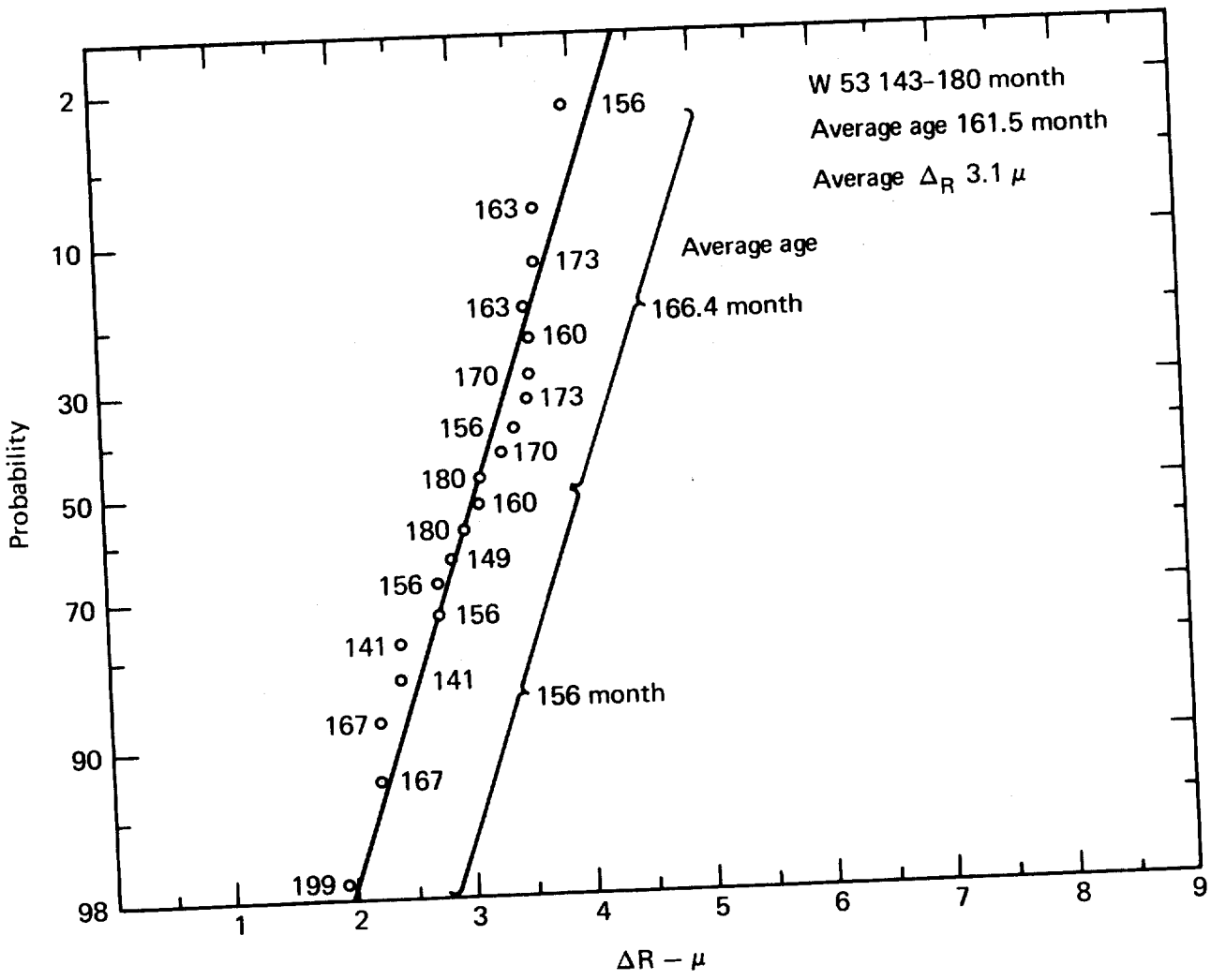
W 53 143-180 month
Average age 161.5 month
Average Δ_R 3.1 μ
Average age
166.4 month
156 month
Probability
2
10
30
50
70
90
98
1
2
3
4
5
6
7
8
9
$\Delta R - \mu$
156
163
173
163
160
170
173
156
170
180
160
180
149
156
156
141
141
167
167
199

FIGURE 3A

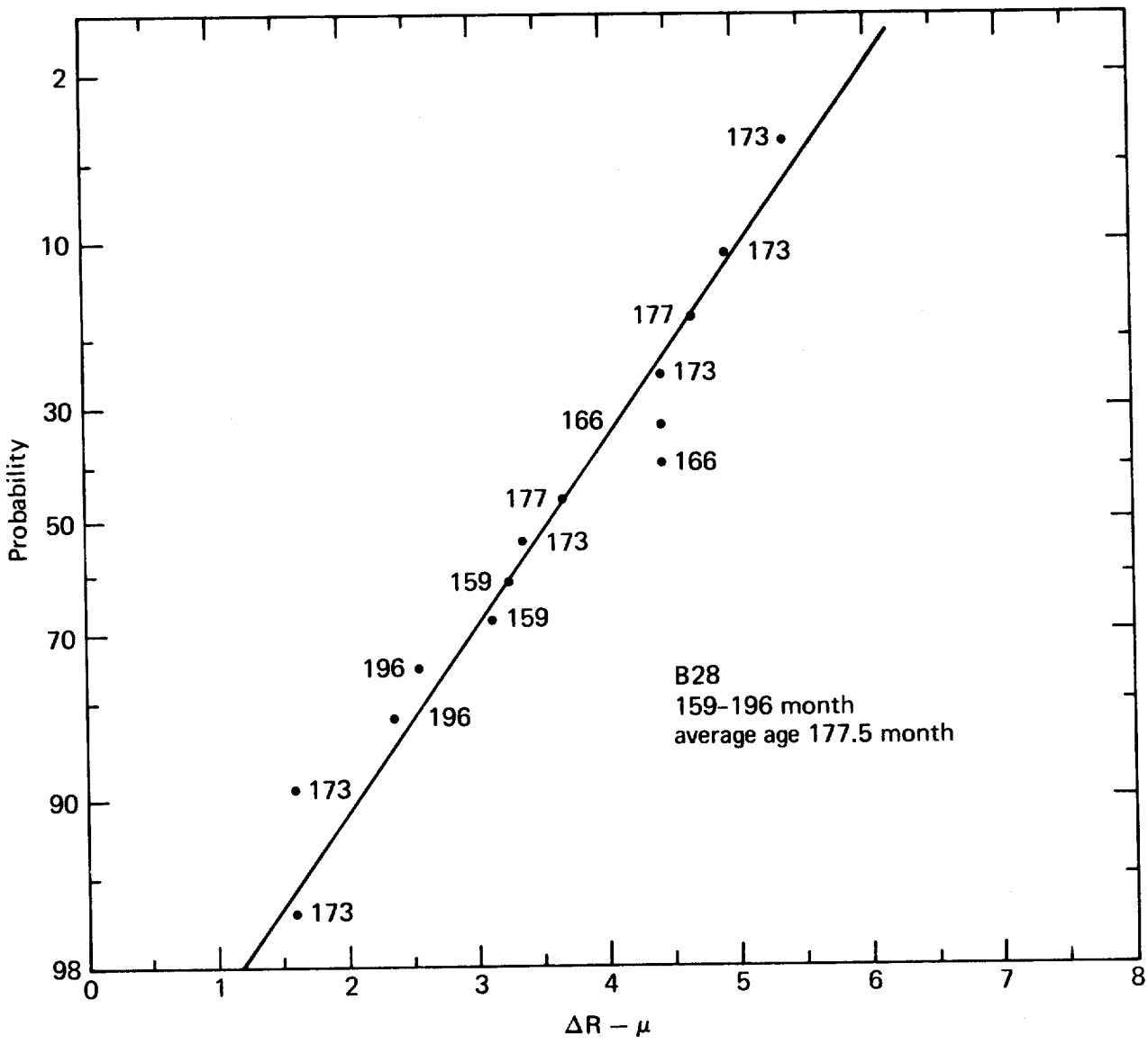
Probability
2
10
30
50
70
90
98
0
1
2
3
4
5
6
7
8
ΔR − μ
173
173
177
173
166
166
177
173
159
159
196
196
173
173
B28
159-196 month
average age 177.5 month

FIGURE 4A

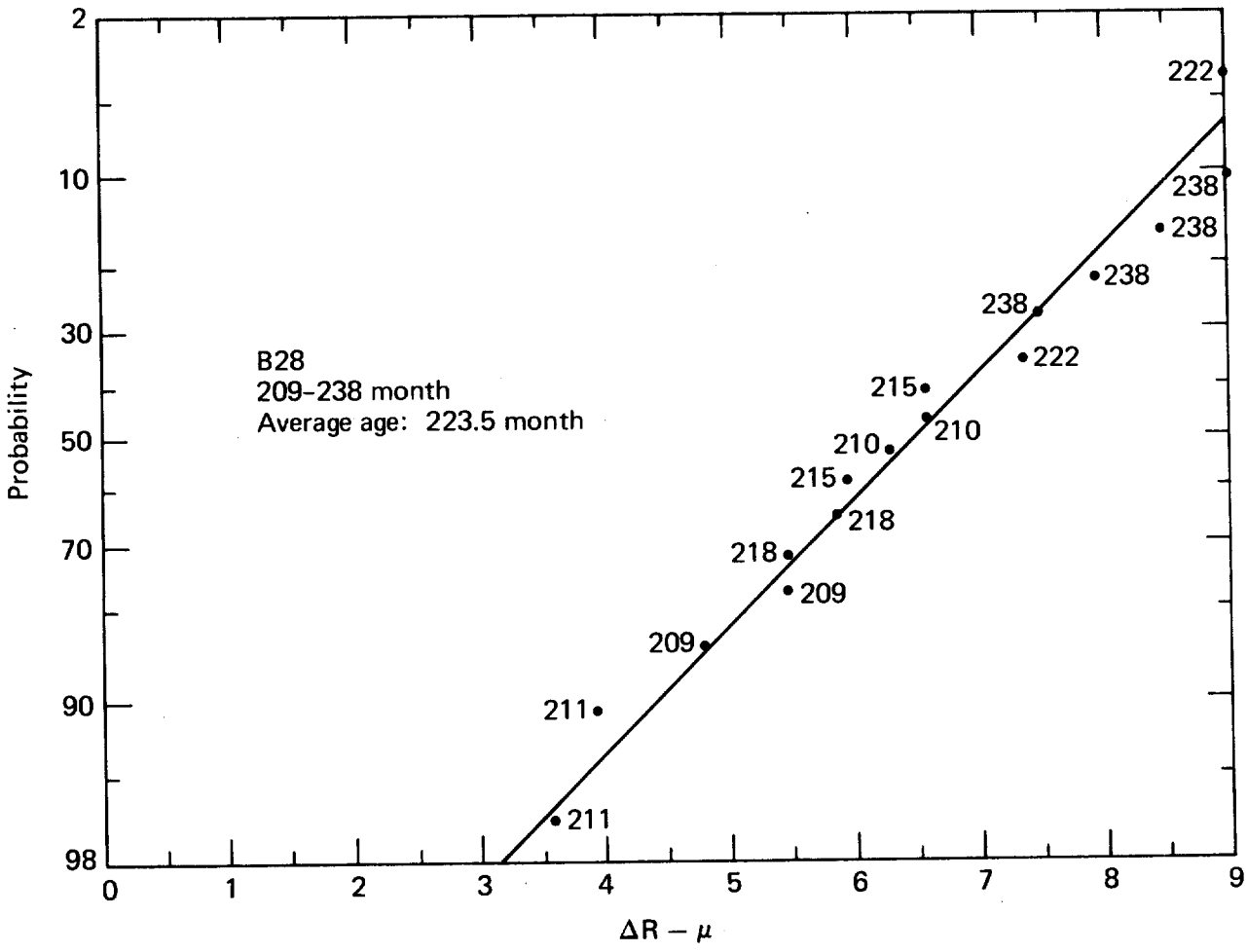
B28
209-238 month
Average age: 223.5 month
Probability
2
10
30
50
70
90
98
0
1
2
3
4
5
6
7
8
9
ΔR − μ
222
238
238
238
238
222
215
210
210
215
218
218
209
209
211
211

FIGURE 5A

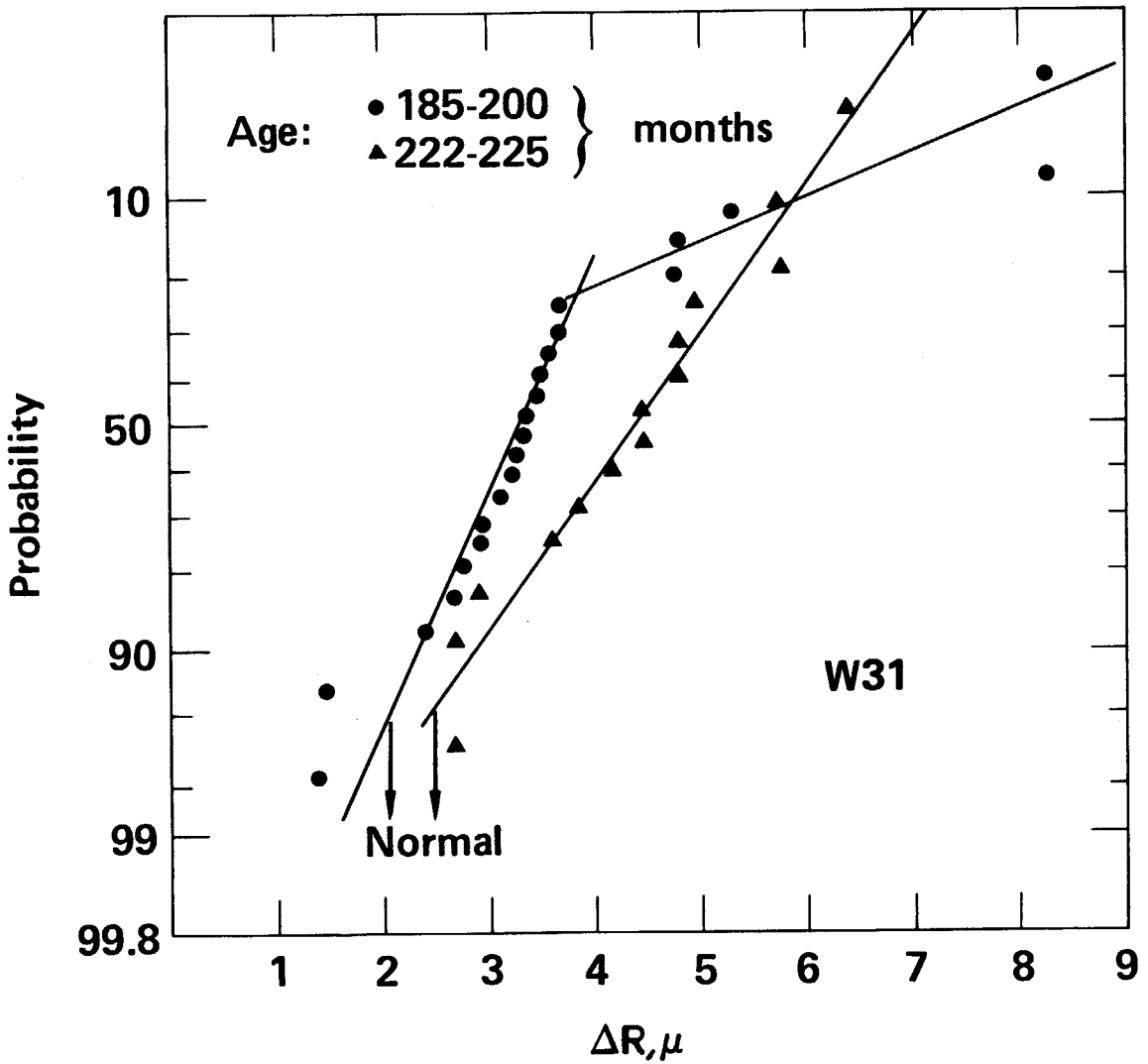
Age:
• 185-200
▲ 222-225
months
10
50
90
99
99.8
Probability
W31
Normal
1
2
3
4
5
6
7
8
9
ΔR, μ

FIGURE 6A

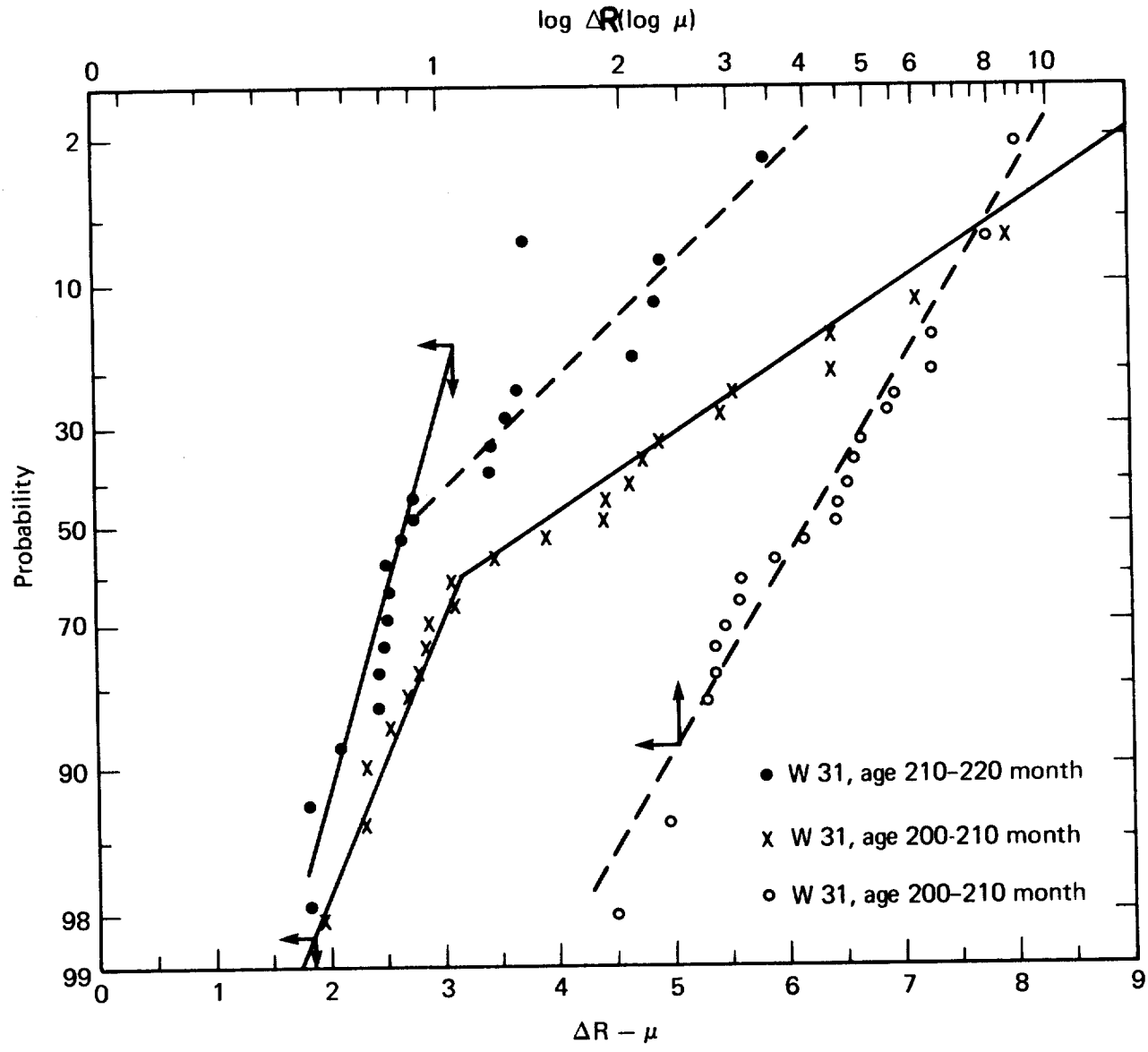
log ΔR(log μ)
0
1
2
3
4
5
6
8
10
2
10
30
50
70
90
98
99
Probability
0
1
2
3
4
5
6
7
8
9
ΔR − μ
W 31, age 210–220 month
W 31, age 200-210 month
W 31, age 200–210 month

FIGURE 7A

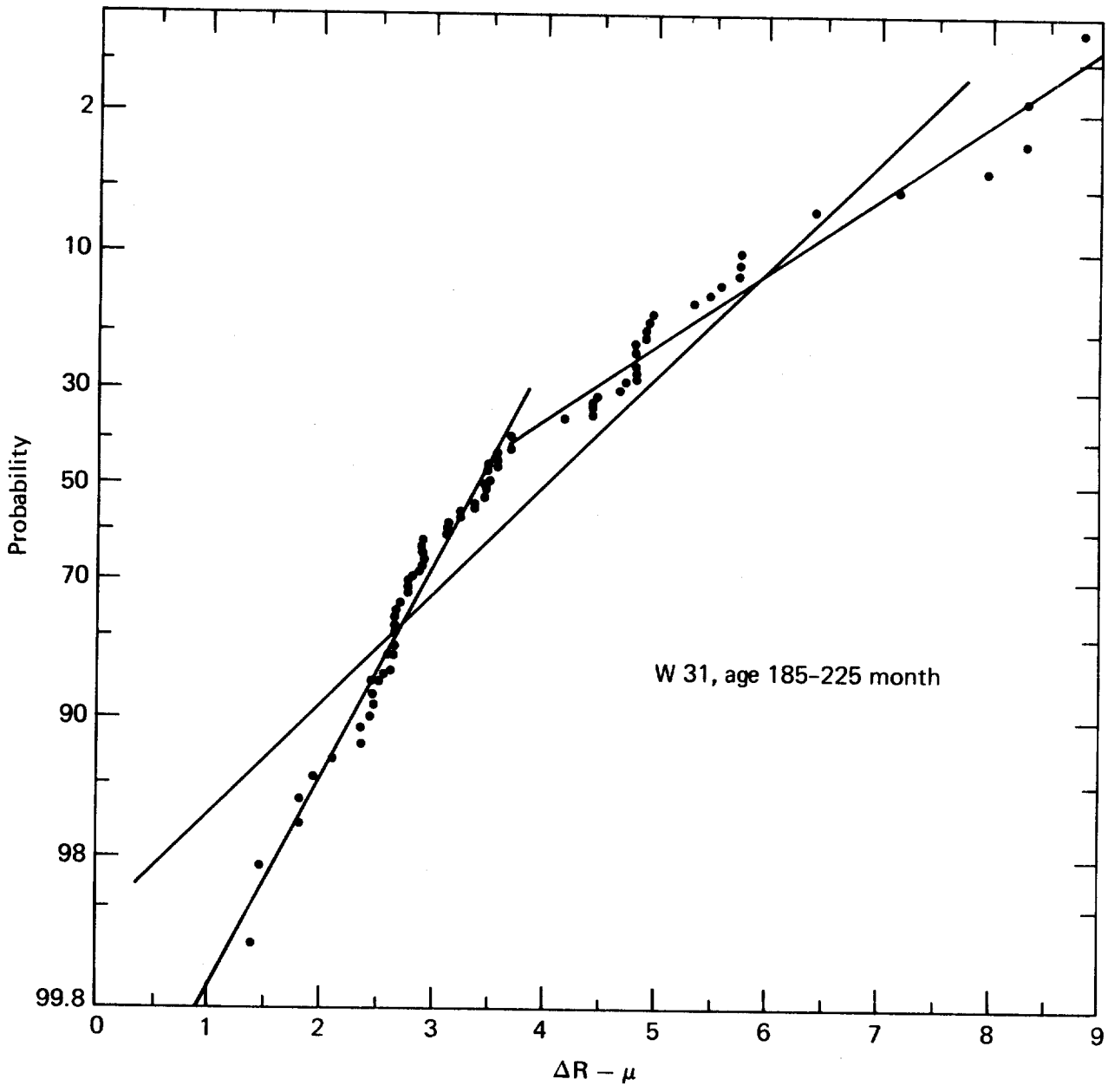
Probability
2
10
30
50
70
90
98
99.8
0
1
2
3
4
5
6
7
8
9
ΔR − μ
W 31, age 185-225 month

FIGURE 8A

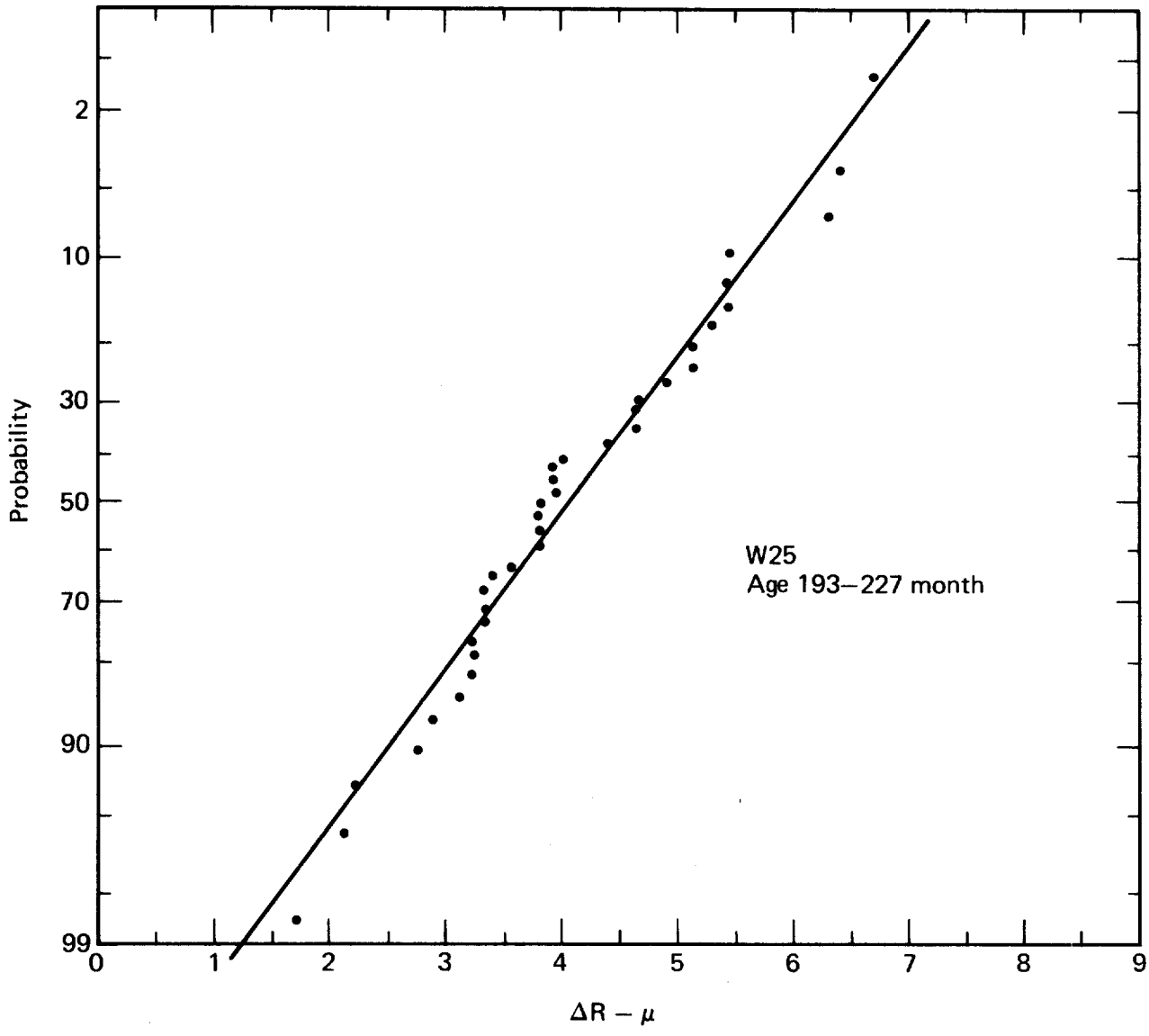
Probability
2
10
30
50
70
90
99
0
1
2
3
4
5
6
7
8
9
ΔR − μ
W25
Age 193–227 month

FIGURE 9A

LINEAR LEAST SQUARES FIT OF DECREASE IN GOLD BRIDGEWIRE RADIUS VERSUS TIME OVER DATA RANGE

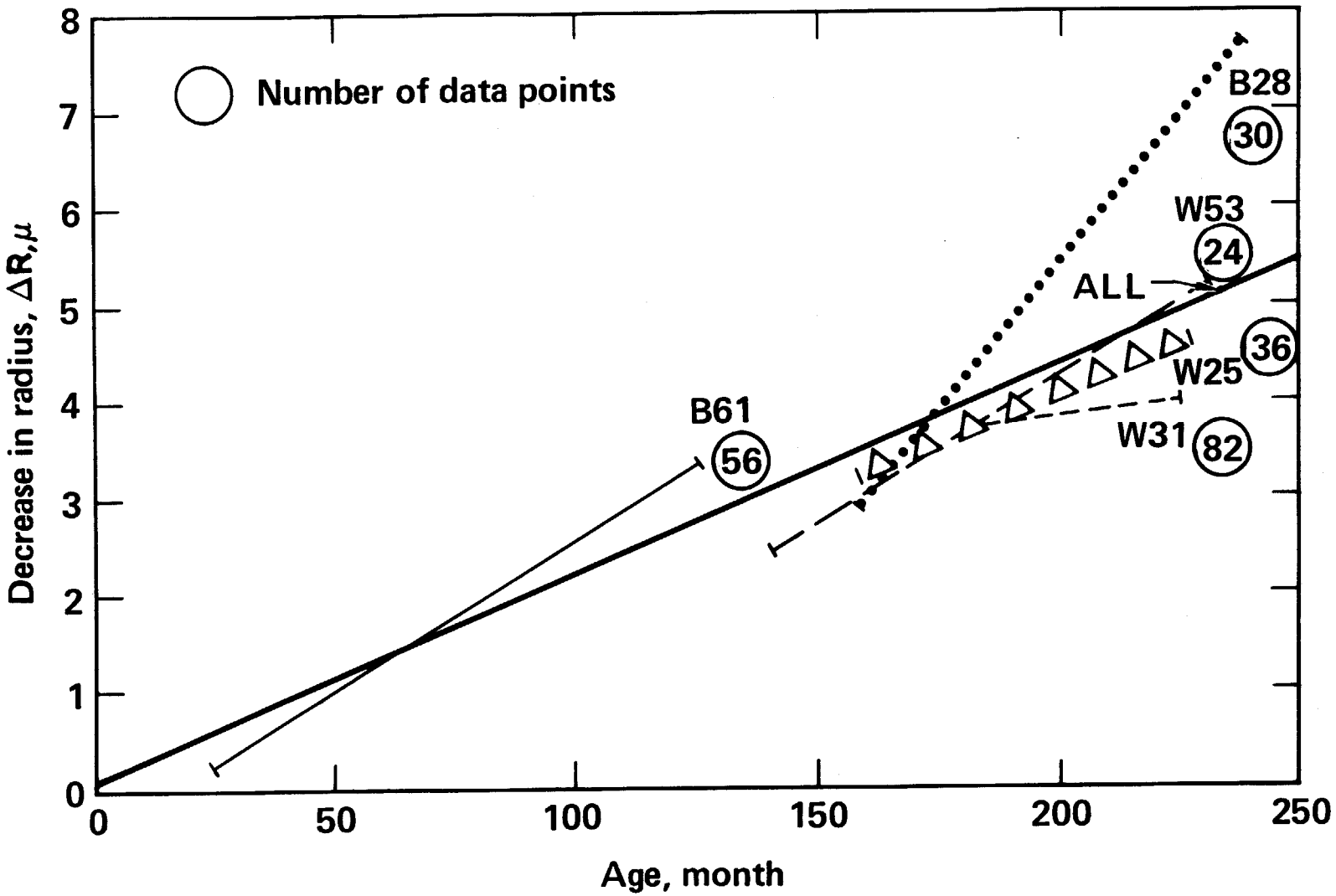

FIGURE 10A

LINEAR LEAST SQUARES FIT OF DECREASES IN GOLD BRIDGEWIRE RADIUS VERSUS SQUARE ROOT OF TIME OVER DATA RANGE

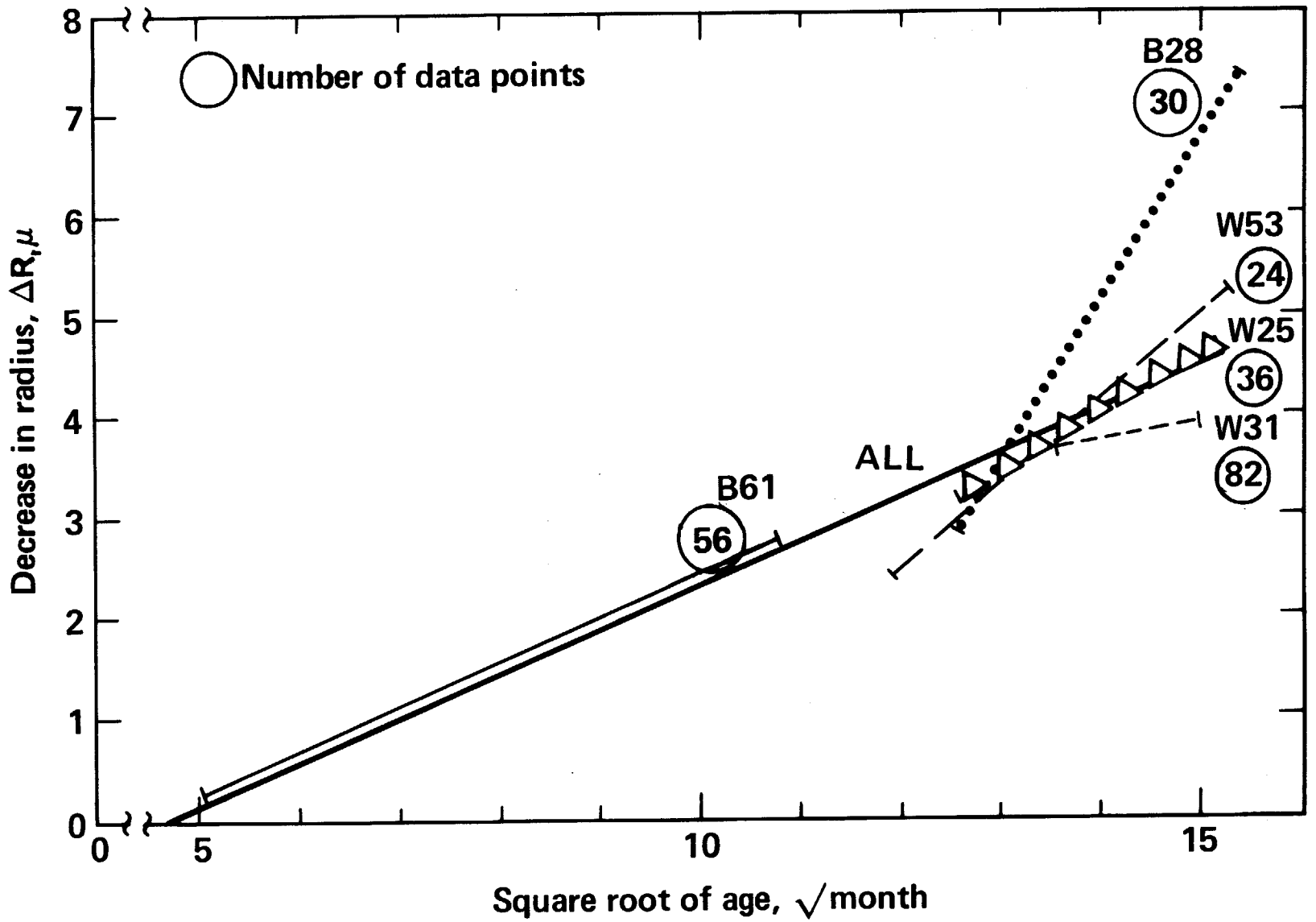

FIGURE 11A

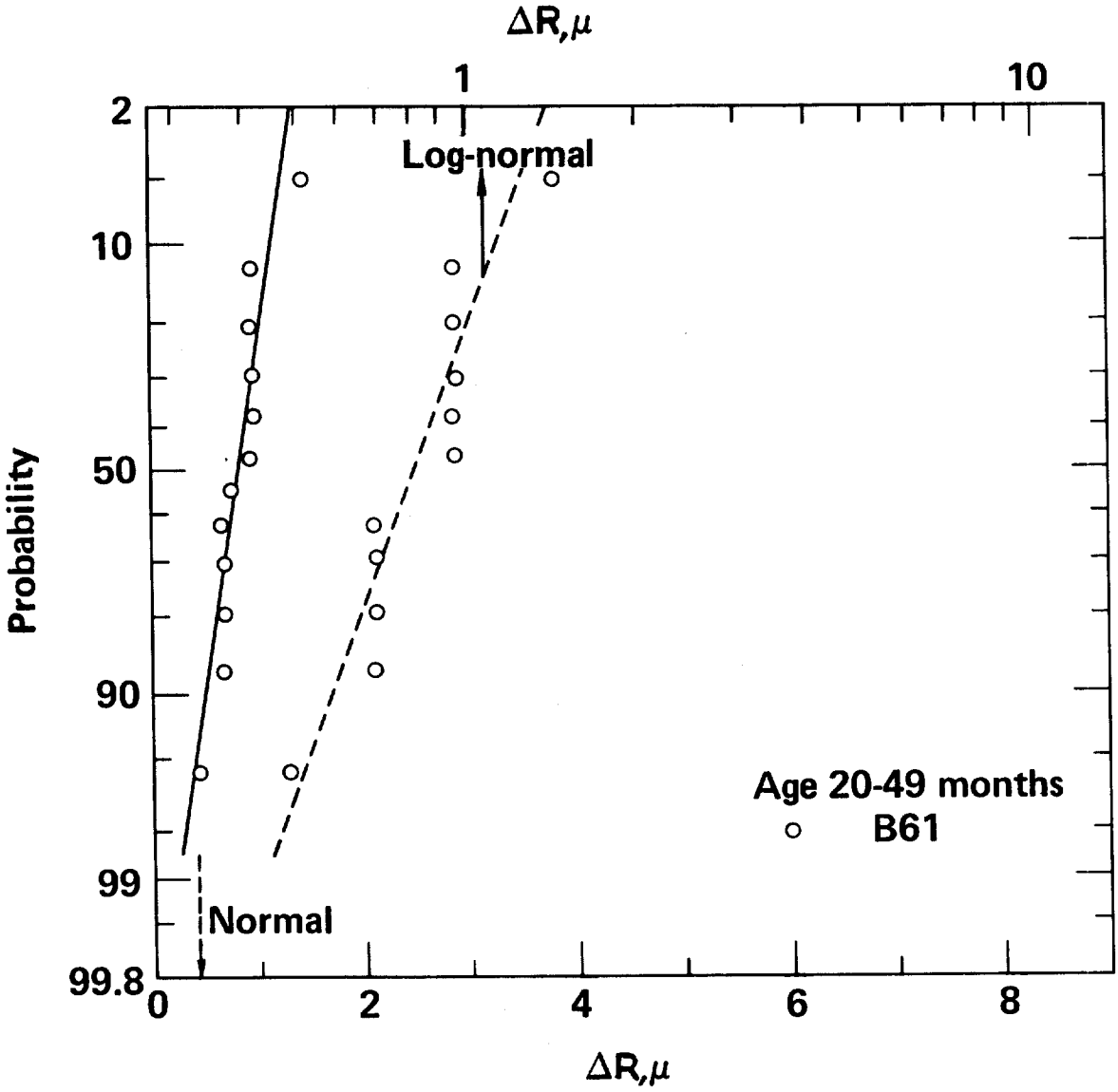
ΔR,μ
1
10
2
10
50
90
99
99.8
Probability
Log-normal
Normal
Age 20-49 months
B61
0
2
4
6
8
ΔR,μ

FIGURE 12A

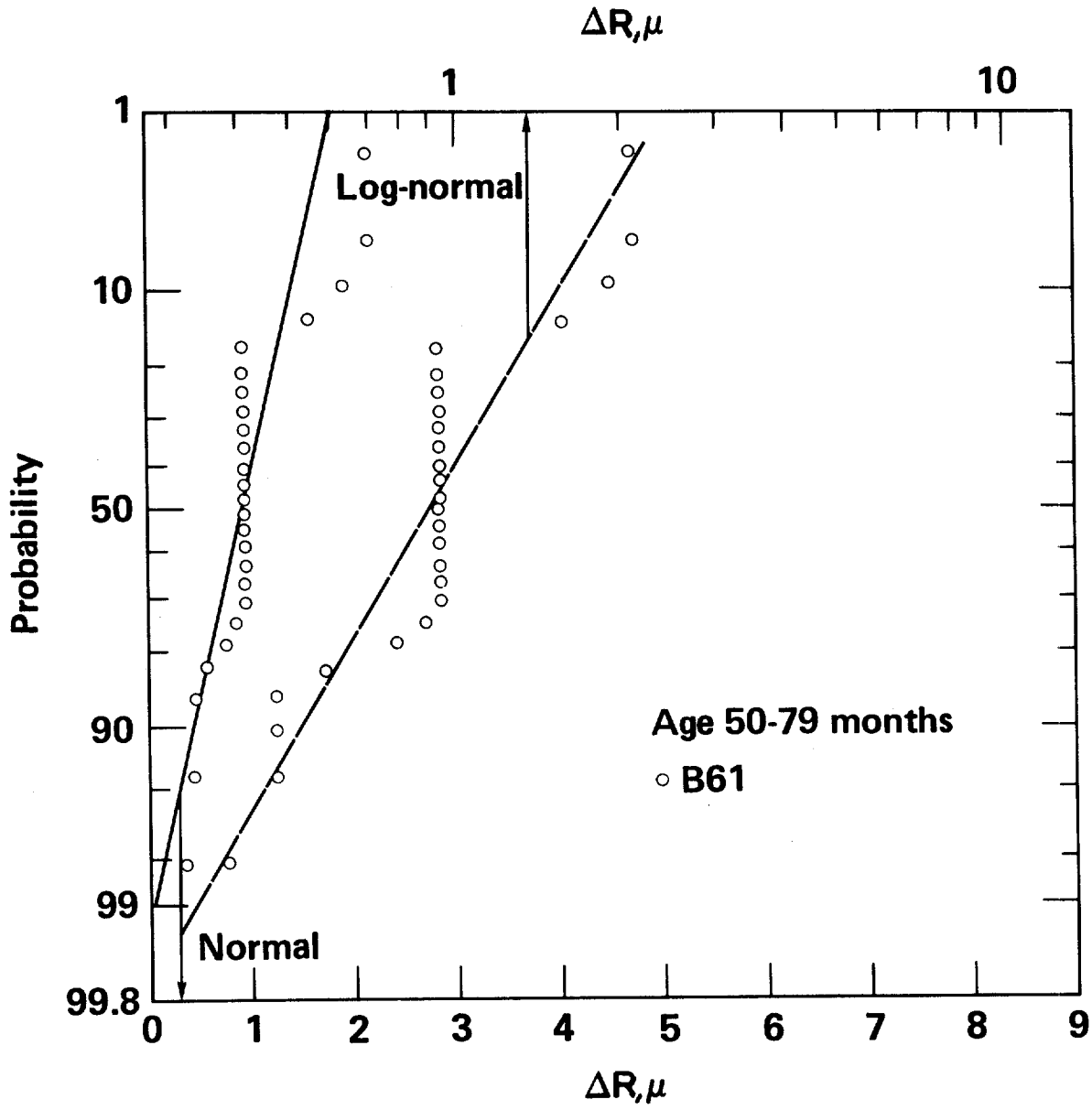
ΔR,μ
1
10
1
10
50
90
99
99.8
Probability
Log-normal
Normal
Age 50-79 months
B61
0
1
2
3
4
5
6
7
8
9
ΔR,μ

FIGURE 13A

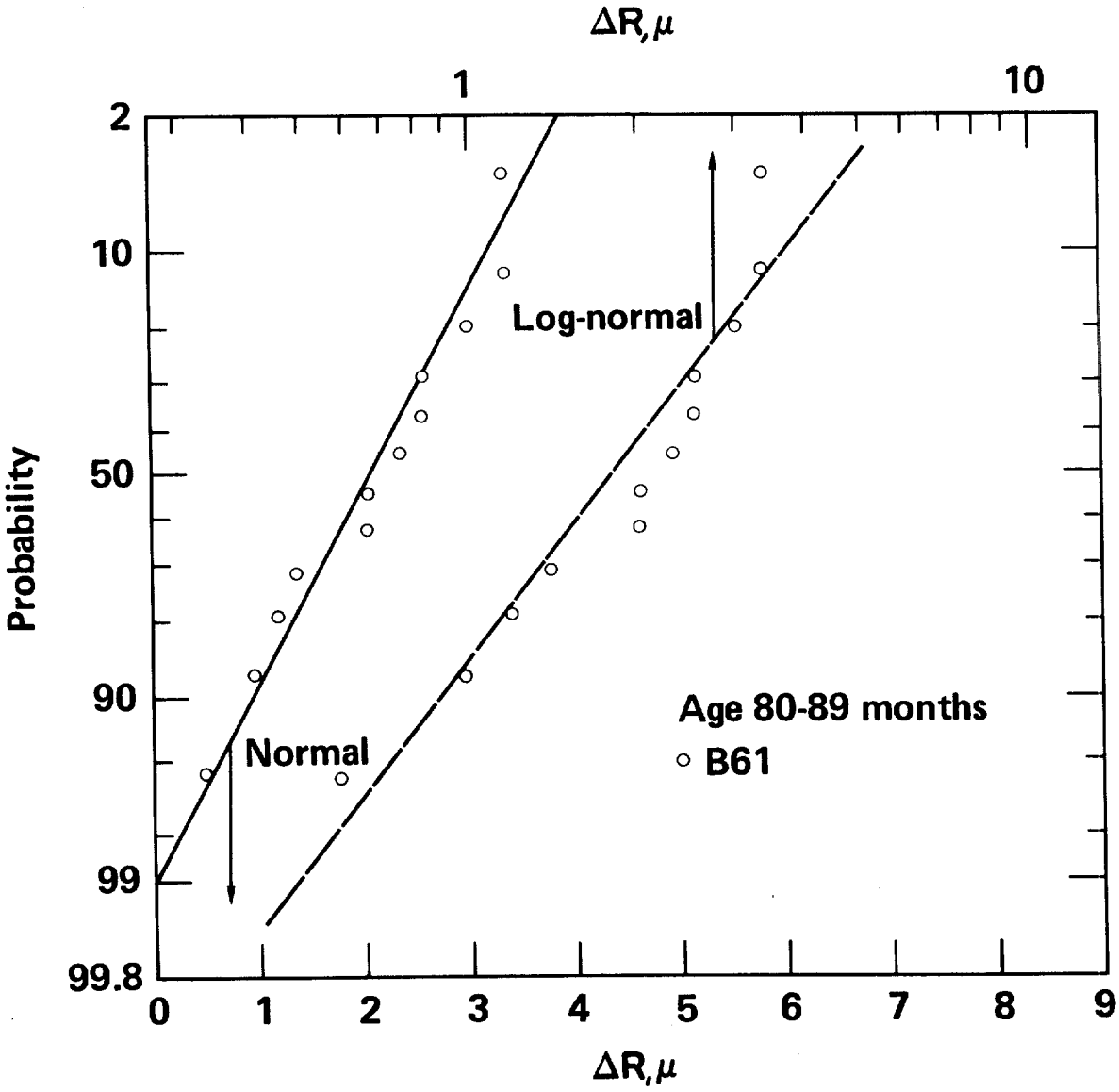
ΔR,μ
1
10
2
10
50
90
99
99.8
Probability
Log-normal
Normal
Age 80-89 months
B61
0
1
2
3
4
5
6
7
8
9
ΔR,μ

FIGURE 14A

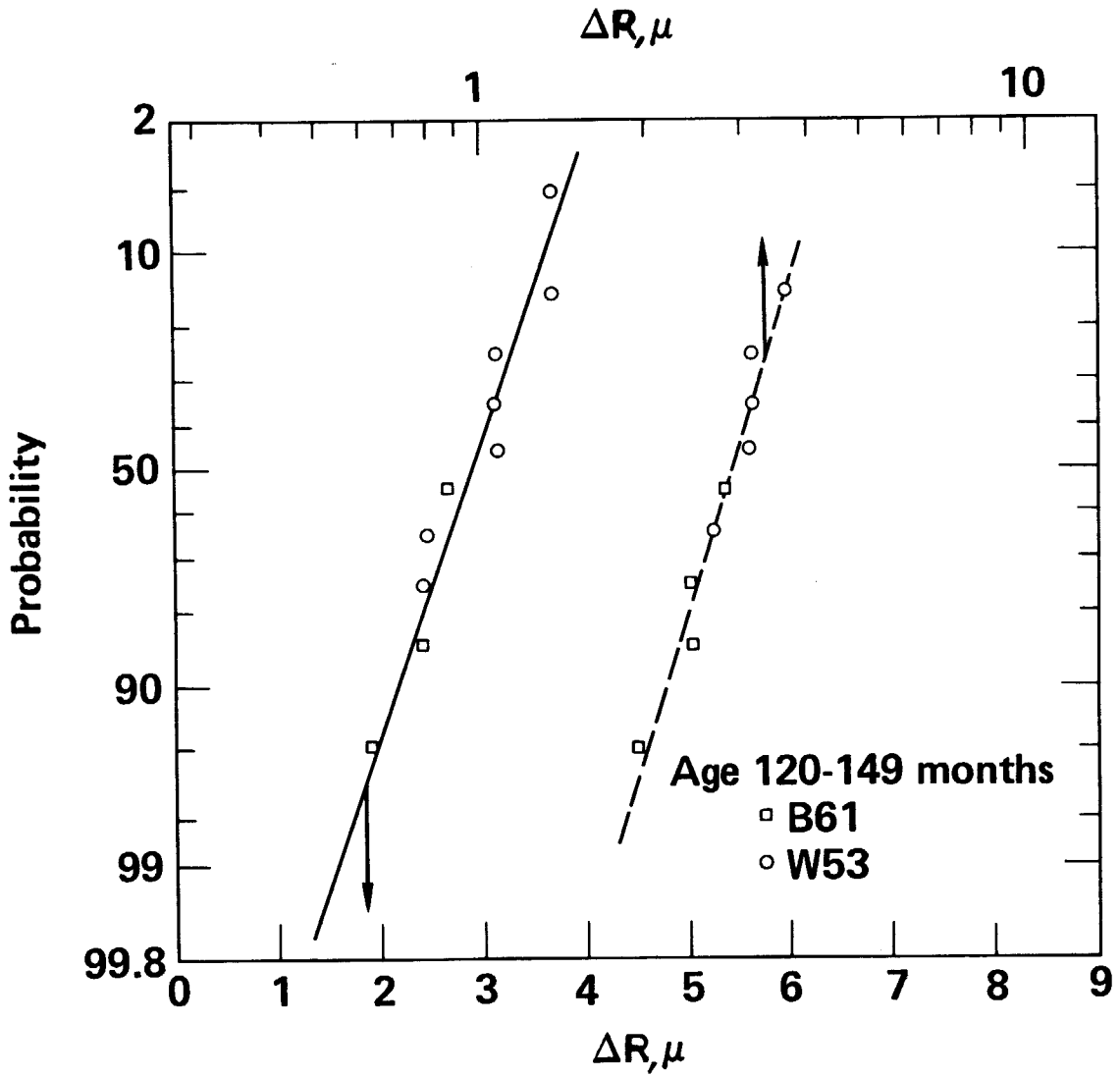
ΔR,μ
1
10
2
10
50
90
99
99.8
Probability
0
1
2
3
4
5
6
7
8
9
ΔR,μ
Age 120-149 months
B61
W53

FIGURE 15A

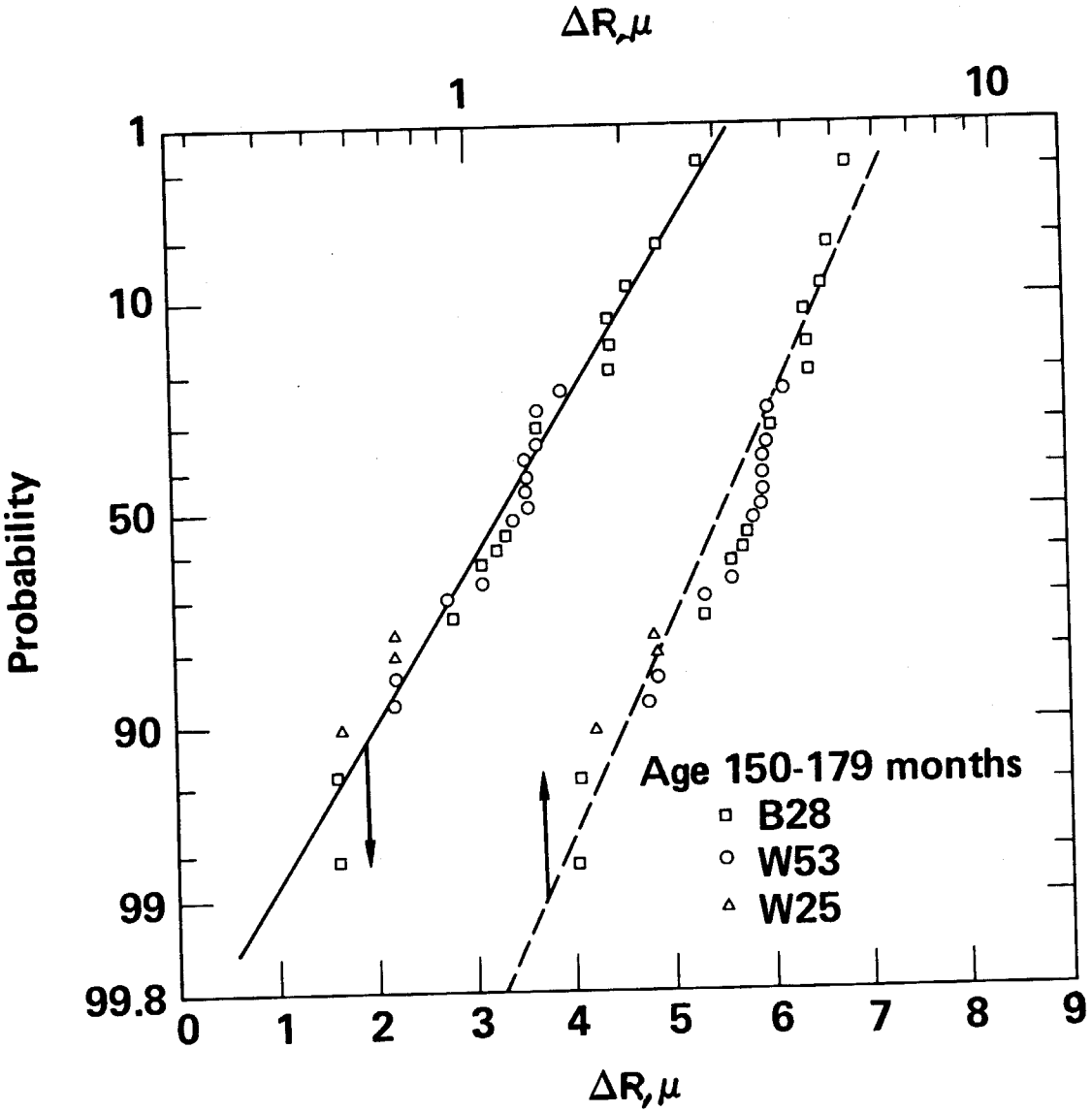
ΔR, μ
1
10
Probability
1
10
50
90
99
99.8
0
1
2
3
4
5
6
7
8
9
ΔR, μ
Age 150-179 months
B28
W53
W25

FIGURE 16A

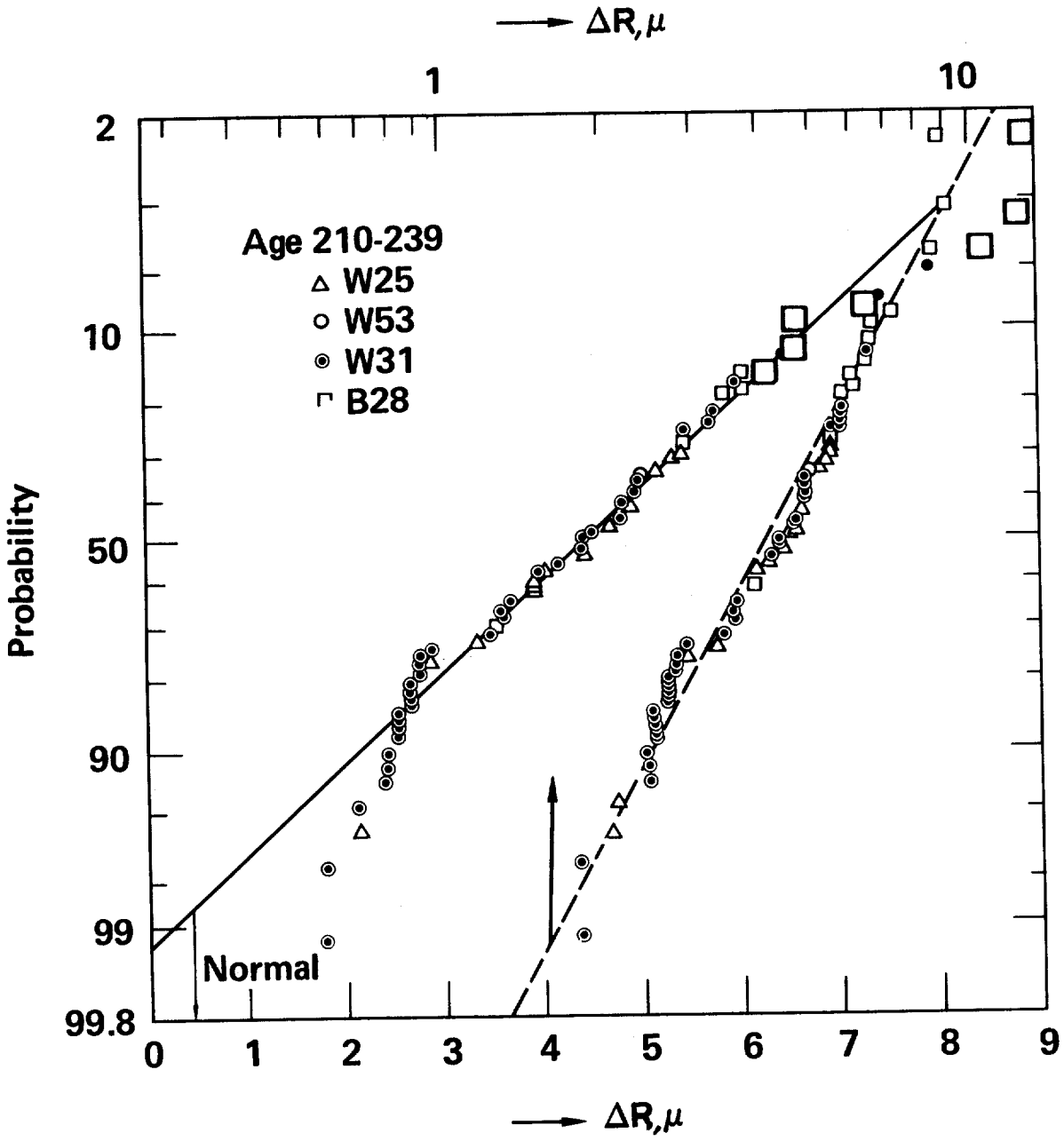
ΔR,μ
1
10
2
10
50
90
99
99.8
Probability
Age 210-239
W25
W53
W31
B28
Normal
0
1
2
3
4
5
6
7
8
9
ΔR,μ

FIGURE 17A

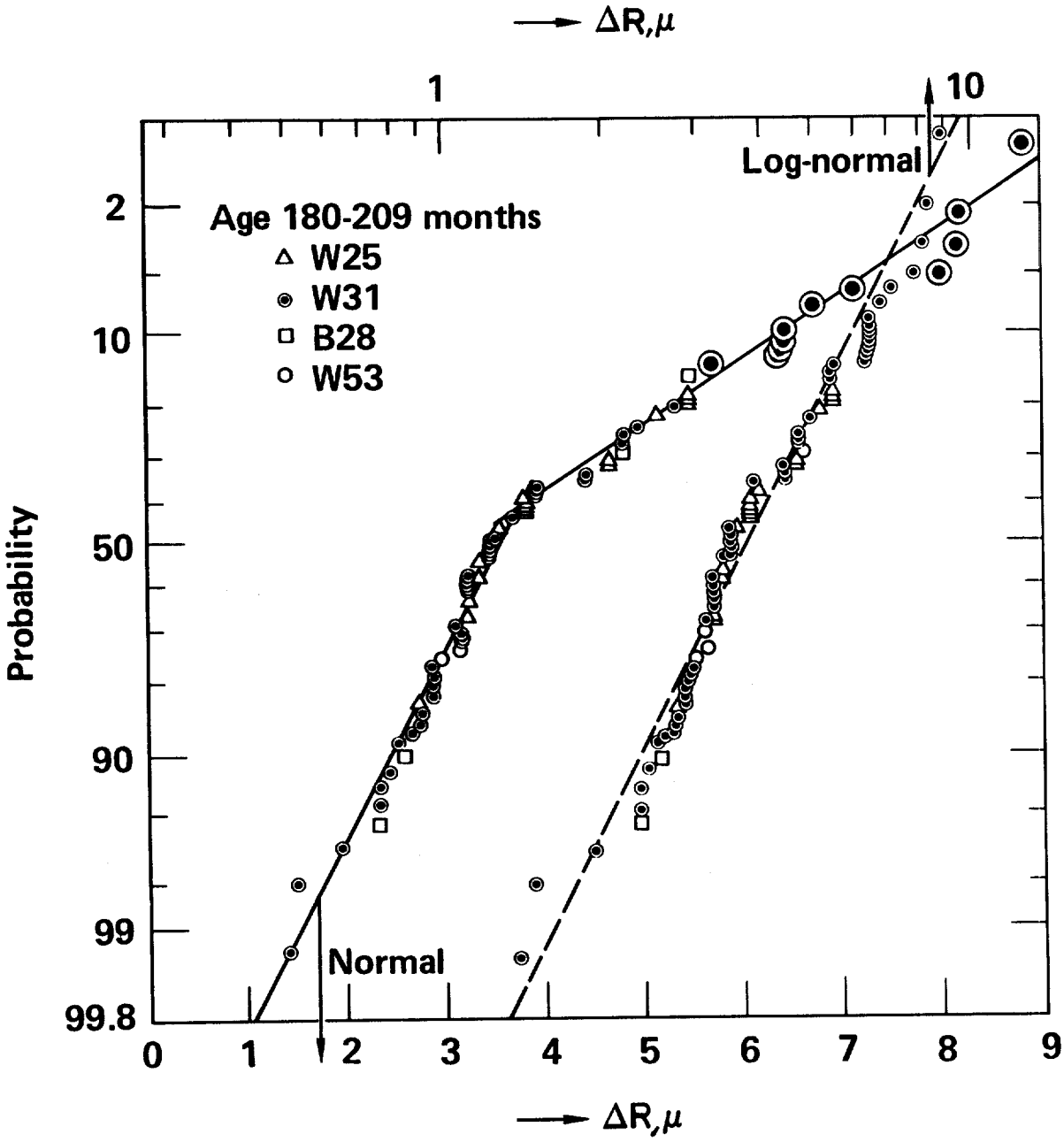
ΔR,μ
1
10
Log-normal
Age 180-209 months
W25
W31
B28
W53
Probability
2
10
50
90
99
99.8
Normal
0
1
2
3
4
5
6
7
8
9
ΔR,μ

FIGURE 18A

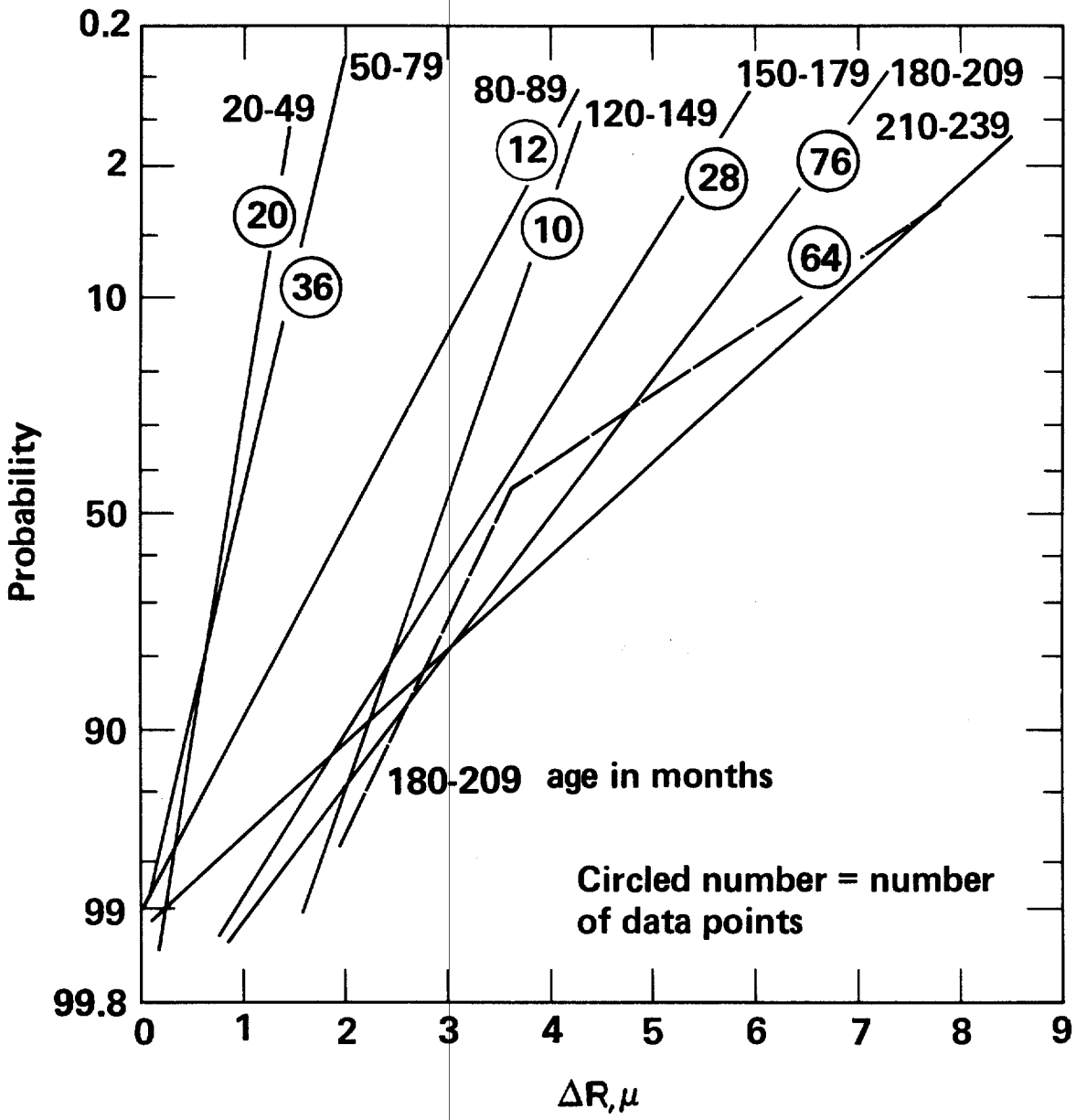
0.2
2
10
50
90
99
99.8
Probability
0
1
2
3
4
5
6
7
8
9
ΔR, μ
20-49
50-79
80-89
120-149
150-179
180-209
210-239
20
36
12
10
28
76
64
180-209 age in months
Circled number = number of data points

FIGURE 19A

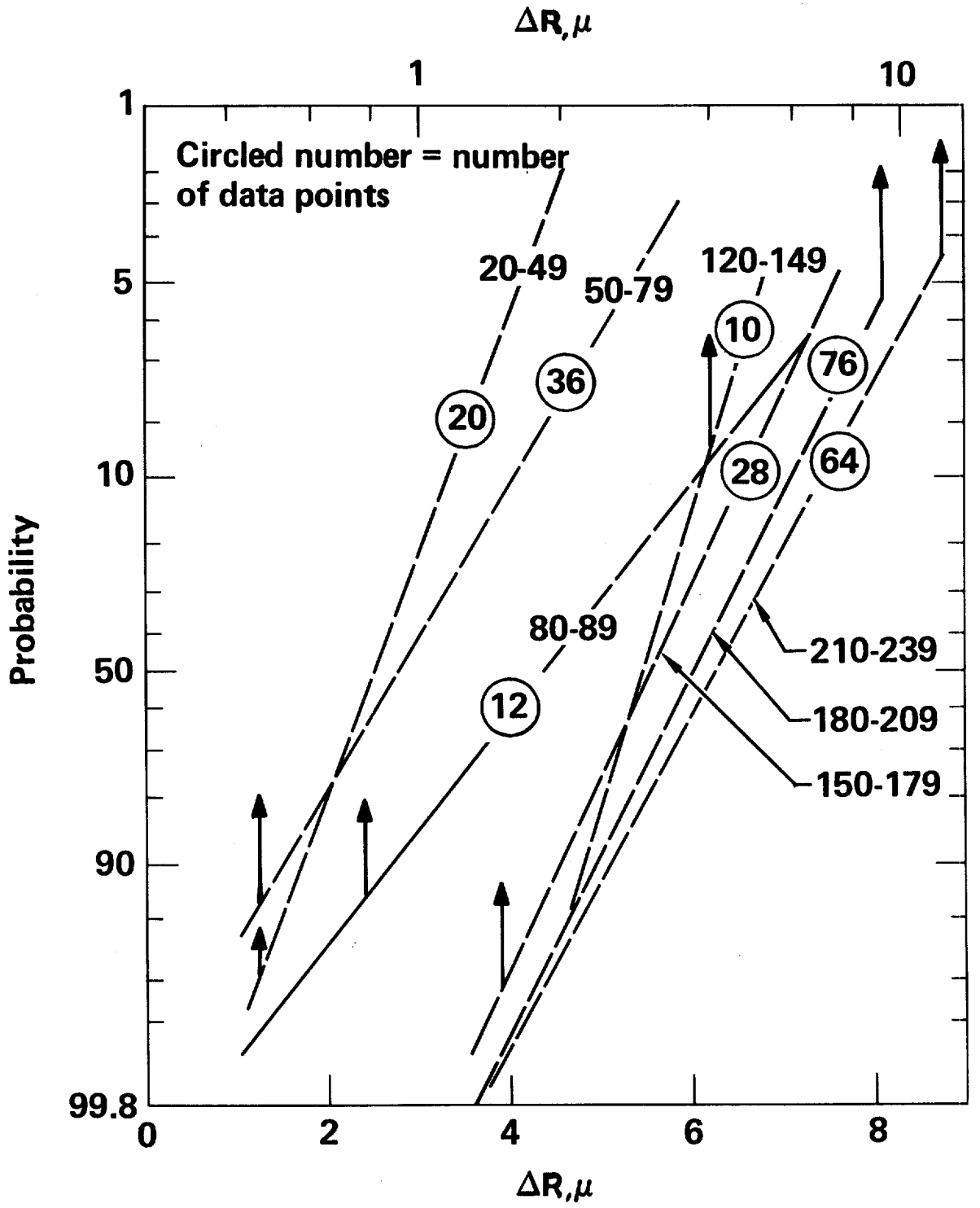
ΔR, μ
1
10
Circled number = number of data points
20-49
50-79
120-149
20
36
10
76
28
64
80-89
12
210-239
180-209
150-179
Probability
1
5
10
50
90
99.8
0
2
4
6
8
ΔR, μ

FIGURE 20A

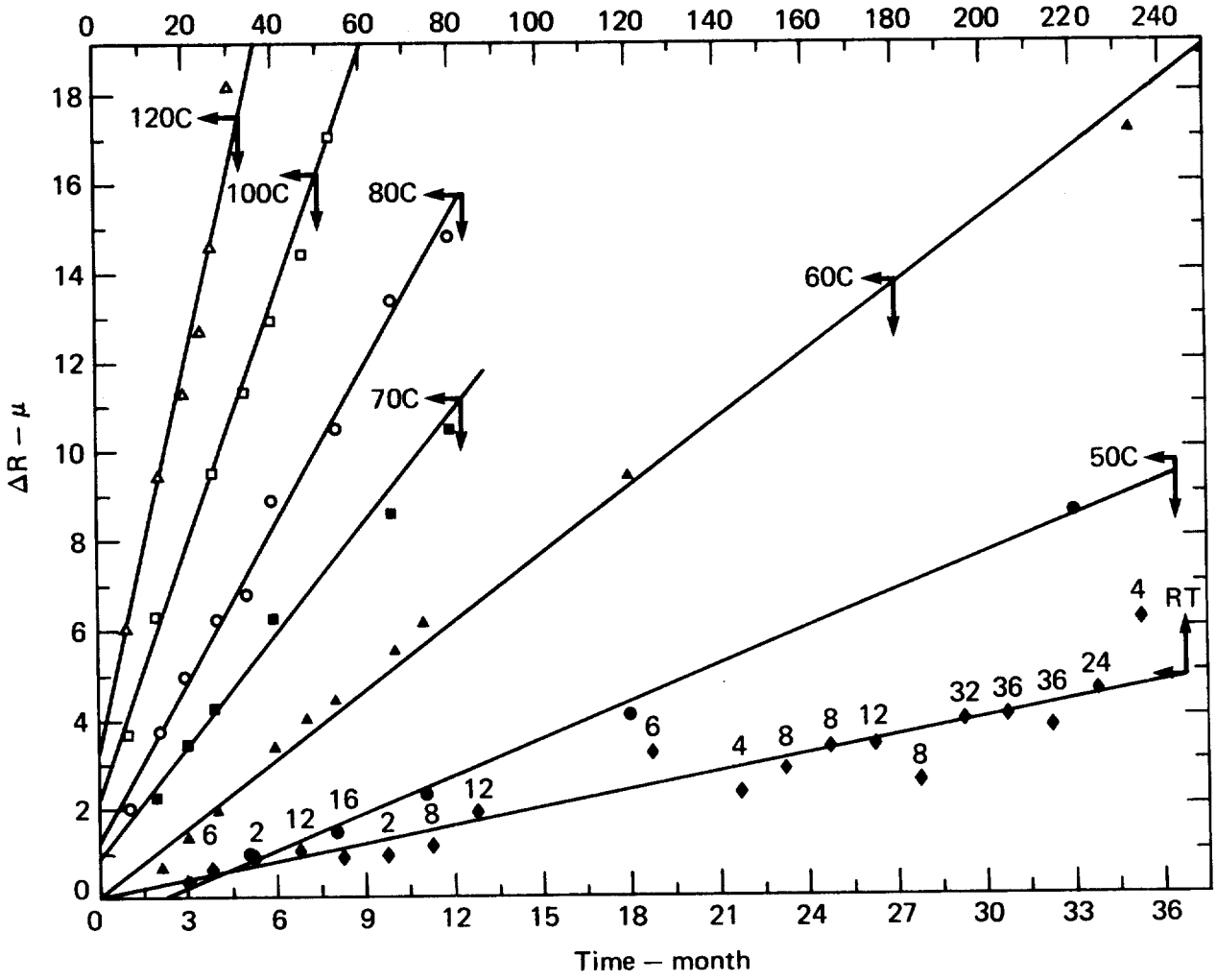
0 20 40 60 80 100 120 140 160 180 200 220 240
18
16
14
12
10
8
6
4
2
0
ΔR – μ
120C
100C
80C
70C
60C
50C
RT
4
6
2
12
16
2
8
12
6
4
8
8
12
8
32
36
36
24
0 3 6 9 12 15 18 21 24 27 30 33 36
Time – month

FIGURE 21A

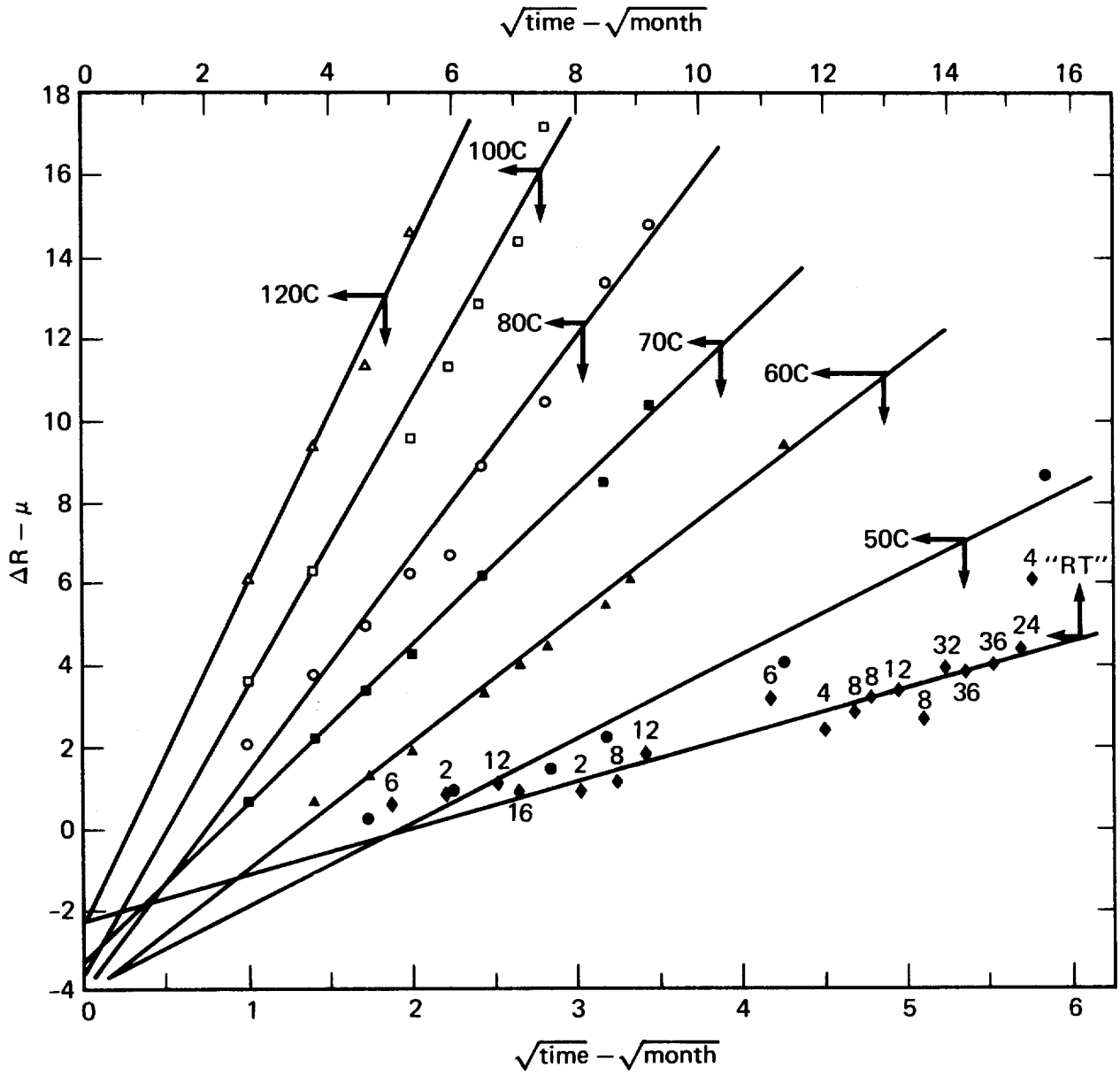
√time − √month
0
2
4
6
8
10
12
14
16
18
100C
120C
80C
70C
60C
50C
4 "RT"
ΔR − μ
-4
-2
0
2
4
6
8
10
12
14
16
1
3
5
6
12
2
8
16
32
36
24

FIGURE 22A

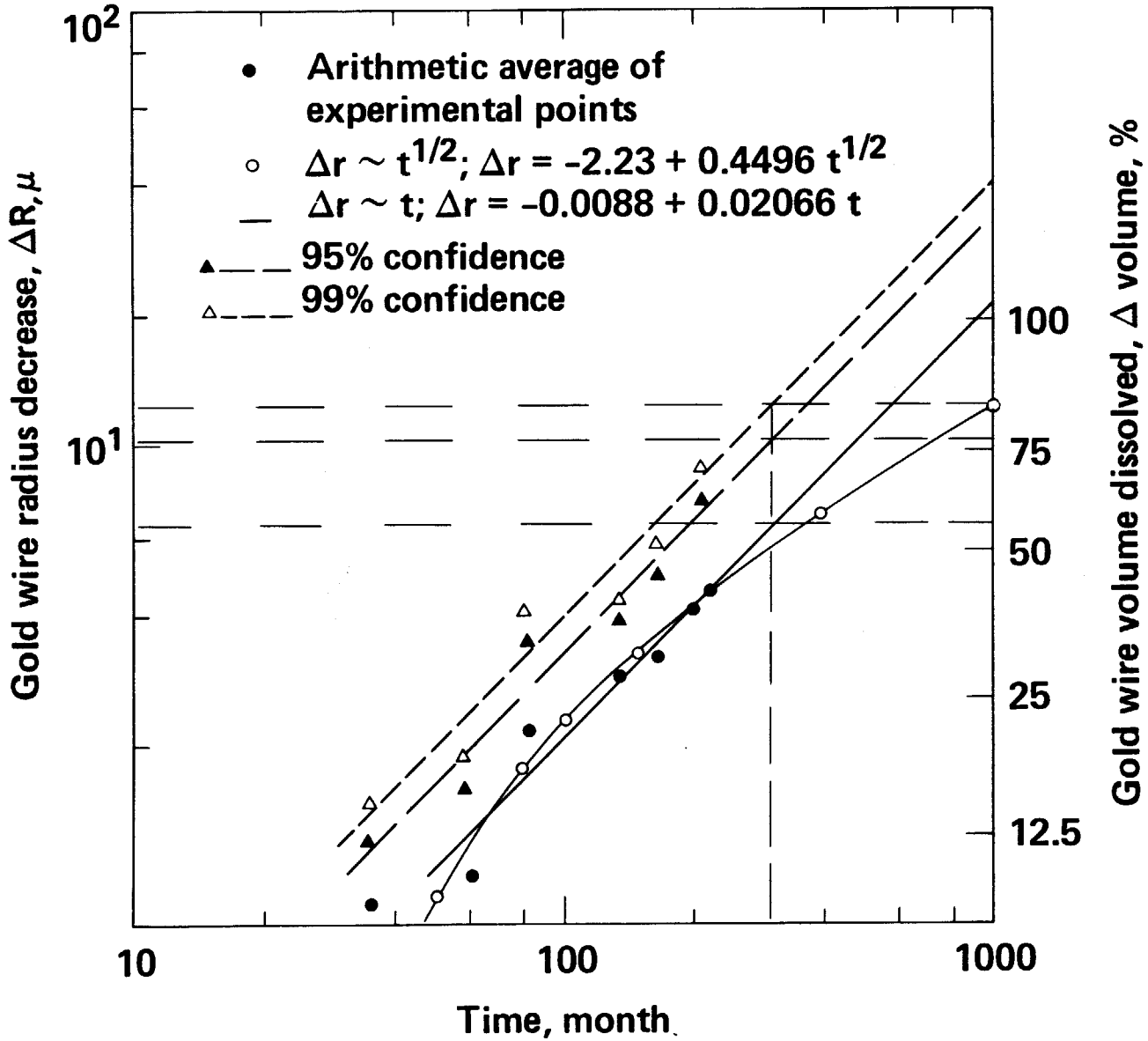
Arithmetic average of experimental points
$\Delta r \sim t^{1/2}$; $\Delta r = -2.23 + 0.4496\ t^{1/2}$
$\Delta r \sim t$; $\Delta r = -0.0088 + 0.02066\ t$
95% confidence
99% confidence
10^2
10^1
Gold wire radius decrease, $\Delta R, \mu$
100
75
50
25
12.5
Gold wire volume dissolved, Δ volume, %
10
100
1000
Time, month

FIGURE 23A